esa

DOCUMENT

document title/ titre du document

ECHO

ENVIRONMENTAL SPECIFICATION

prepared by/*préparé par* J. Sørensen

reference/*réference* JS-1-12
issue/*édition* 1
revision/*révision* 0
date of issue/*date d'édition* 12 January 2012
status/*état*
Document type/*type de document*
Distribution/*distribution*

European Space Agency
Agence spatiale européenne

ESTEC
European Space Research and Technology Centre - Keplerlaan 1 - 2201 AZ Noordwijk - The Netherlands
Tel. (31) 71 5656565 - Fax (31) 71 5656040 www.esa.int

APPROVAL

Title *Titre*	EChO Environmental Specification	issue 1 *issue*	revision 0 *revision*

author *auteur*	J. Sørensen
date *date*	

approved by *approuvé par*	
date *date*	

CHANGE LOG

reason for change */raison du changement*	issue/*issue*	revision/*revision*	date/*date*
Initial issue	1	0	12/1-2012

CHANGE RECORD

Issue: 1 Revision: 0

reason for change/*raison du changement*	page(s)/*page(s)*	paragraph(s)/*paragraph(s)*

TABLE OF CONTENTS

1 INTRODUCTION

The space environment presents a major problem to all spacecraft including EChO. Proper assessment of the potential effects is an essential part of the engineering process leading to the construction of any element of the spacecraft. It is important that this is taken into account from the earliest phases of a project when consideration is given to mass budget, protection, component selection policy, etc. As the design of an element is developed, further engineering iteration is normally necessary with more detailed analysis.

This document is prepared for study of the EChO mission. It is intended to assist the developers of instruments for the mission to asses the effects of the space environment on their systems. The document is based on the ECSS Space Environment Standard RD[1], from which most of the background information has been taken (ECSS is a cooperative effort of the European Space Agency, National Space Agencies and European industry associations for the purpose of developing and maintaining common standards). This standard shall apply to all space environments and effects analyses. It defines appropriate analysis methods and models, including the ones employed here.

1.1 The Mission

The overall objective of the EChO (Exoplanet Characterisation Observatory) mission is to characterise the atmospheres of nearby transiting exoplanets.

The baseline operational orbit of the EChO spacecraft is a large halo orbit around the 2nd Lagrangian (L2) point. This virtual point in space is located about 1.5million km from the Earth in the anti-Sun direction, and is becoming the orbit of choice of many future astronomical missions, because it offers the possibility of long uninterrupted observations in a, in many aspects, fairly stable environment (thermal, radiation etc.). The spacecraft will be launched by a Soyuz rocket from Kourou. A direct escape injection is expected. The nominal mission duration is 5years. An extended mission with minimum duration of an additional 1year is foreseen. The spacecraft shall be designed for the extended mission. The data presented in this document are therefore valid for a total mission duration of 6 years.

1.2 The Environment

In general, when assessing the effects of the space environment on an instrument, the following environments should be included:

- Magnetic field
- Solar and Planetary Electromagnetic Radiation
- Neutral Atmosphere
- Plasmas
- Energetic Particle Radiation
- Particulates
- Contamination

In the following each component of the space environment, except the magnetic field and the neutral atmosphere, is treated separately, although synergies and cross-linking of models are specified. The natural environment is described together with the general models in use and principles for determining the local induced environment. Although important, especially in driving the energetic particle radiation, the magnetic field is not described separately here. Since the EChO orbit is well outside the atmosphere, the neutral atmosphere is not described in this document either.

Each environment is treated in a separate chapter. Some of the models mentioned are also installed in the Space Environment Information System (SPENVIS) RD[2].

For many of the associated analyses it is necessary to take the geometry of the spacecraft into account, but such geometrical analyses are out of the scope of this document.

2 SOLAR AND PLANETARY ELECTROMAGNETIC RADIATION

2.1 Introduction

In general spacecraft receive electromagnetic radiation from several external sources. The largest source is generally the direct solar flux. The fraction of incident sunlight that is reflected off a planet is termed albedo. When in orbit around a planet this will also contribute to the flux received by the spacecraft (depending on the sunlit part of the planet, which the spacecraft can see). A third source is the planet-emitted infrared radiation.

The EChO spacecraft is in its operational orbit so far away from the Earth that the albedo and the planet infrared radiation can be ignored, and only the direct solar flux needs to be taken into account. Furthermore the orbit around L2 is designed such, that the spacecraft stays away from the zone, where the Sun is eclipsed by the Earth, during the entire mission.

The electromagnetic radiation varies with solar activities, which is highly variable over a solar cycle. The given data are mainly average values. For thermal analyses or certain special applications more detailed treatment may be required, which is outside the scope of this document.

2.2 Solar electromagnetic radiation

2.2.1 DIRECT SOLAR FLUX

The direct solar flux is inverse proportional to the square of the distance to the Sun. At the Earth's distance the value is fairly constant. The following values for the electromagnetic radiation shall be used (solar energy that falls on a unit area of surface normal to the line from the Sun, per unit time):

Table 2-1: Solar irradiance

	Solar flux [W/m²]		
	Average	**Minimum** (summer solstice)	**Maximum** (winter solstice)
At the Earth	1366	1321	1413
At L2 (EChO operational orbit)	1339	1293	1388

The solar irradiance at the average Earth distance is also called the solar constant.

The average solar irradiance at the Earth has an uncertainty of about ±0.2%.

2.2.2 SOLAR SPECTRUM

The solar spectrum shall be approximated by a black body curve with a characteristic temperature of 5780K (this is the temperature that at 1AU gives the value of the solar constant reported above). A space sink temperature of 3 K shall be assumed.

The UV portion (wavelength, λ,< 300 nm) of the electromagnetic spectrum is of particular importance in determining effects of solar radiation on material properties. The integrated irradiance of the near UV electromagnetic radiation flux (180 nm < λ < 400 nm) is approximately:

Average near UV at the Earth 118 W/m^2

The far UV portion (λ < 180 nm) contributes about 0.023 W/m^2 at the Earth's distance.

Certain parts of the spectrum are varying very much, both, over the 27-day solar rotation period and over the 11-year solar cycle. This variation ranges from about 50 % for the near UV part to a factor 2 for the UV and far UV portions and can reach orders of magnitude for flare X-rays.

Average and worst case irradiance levels for the high-energy spectrum are summarized in Table 2-2. The average values for the Earth's distance were taken from RD[3].

Table 2-2: High-energy solar electromagnetic flux

Type	Wavelength (nm)	At the Earth's distance	
		Average Flux (W/m²)	Worst-Case Flux (W/m²)
Near UV	180-400	118	177
UV	< 180	2.3×10^{-2}	4.6×10^{-2}
UV	100-150	7.5×10^{-3}	1.5×10^{-2}
EUV	10-100	2×10^{-3}	4×10^{-3}
X-Rays	1-10	5×10^{-5}	1×10^{-4}
Flare X-Rays	0.1-1	1×10^{-4}	1×10^{-3}

For design purposes the worst-case values of Table 2-2 shall be used. The fluxes given for flare X-rays are peak values of large flares. For design, one such X-ray flare per week, lasting one hour, shall be assumed. More details on the solar spectrum can be found in RD[1] and on the X-ray part of the spectrum in particular in RD[4]. The above values for the Earth's distance shall also be applied for L2.

2.3 Directional and temporal variation

Apart from the global long term variation, the solar irradiation seen by a spacecraft element also varies with the direction in which the element is pointing.

To get the actual incident irradiation seen by an experiment, the shading by other elements of the spacecraft itself also has to be taken into account. For this a geometrical model is needed, which can simulate the pointing in the orbit and the kinematics of the spacecraft.

3 PLASMAS

3.1 Introduction

A plasma is a partly or wholly ionised gas whose particles exhibit collective response to magnetic and electric fields. The collective motion is brought about by the electrostatic Coulomb force between charged particles.
The plasma regimes experienced by the EChO spacecraft are the **solar wind** and the **outer magnetosphere.** The spacecraft can be expected to spend a significant amount of time in both of these regimes.

The principal spacecraft engineering concerns for the EChO spacecraft caused by space plasmas are outlined in Table 3-1.

Table 3-1: Main engineering concerns for EChO due to space plasmas

System	Problem
Scientific experiments	Low level positive or negative charging and photoelectrons which interfere with plasma measurements Plasma entry and potential changes in sensitive detectors
Electric Propulsion	Interaction between generated plasma, ambient plasma, and the spacecraft

Remark that general surface charging with following possibly harmful electrostatic discharges is only a problem in earth orbit at high altitude or polar latitude. The potential ranges expected for EChO are not critical and there should be no risk of powerful discharges. However, the ranges may raise concern for specific systems sensitive to potential fluctuations.

In the following the solar wind, the outer magnetosphere plasma environment and the plasma effects will be described.

3.2 The Solar Wind

3.2.1 DESCRIPTION

The solar wind is part of the Corona, the Sun's outer atmosphere. The high temperature of the plasma near the sun causes it to expand outwards against gravity, carrying the solar magnetic field along with it. The solar wind starts at the Sun as a hot dense, slowly moving plasma but accelerates outwards to become cool, rare and supersonic near Mercury and beyond. Most of the solar wind's acceleration takes place near the sun and so the EChO spacecraft will not observe significant differences in velocity as their distance from the Sun varies.

The solar wind velocity typically lies in the range 300-1200km/s. It is generally around 400km/s, but there are frequent high-speed streams with velocities around 700km/s. These streams are more commonly observed around solar minimum and recur generally with a 27-day period. The strong variability of the solar wind is the driving force, putting energy into the magnetosphere and ultimately causing surface charging and radiation effects. More severe but less frequent disturbances in the solar wind can be caused by coronal mass ejections.

At the Earth, the presence of the magnetopause causes the supersonic solar wind to decelerate abruptly i.e. a shock wave is formed. At this " Bow Shock" the solar wind is slowed, compressed, heated and deflected. The magnetopause is situated about 10 Earth radii upstream on the Earth-Sun line.

Although solar wind plasma is cold, the ions carry considerable kinetic energy, typically ~1keV for protons and ~4keV for He^{++}. This can result in sputtering from surface materials. In the magnetosheath kinetic energy is lower, but sputtering still occurs.

3.2.2 TYPICAL PARAMETERS

Because the solar wind flows past the planets with negligible modification, unless it encounters the bow shock, it can be considered spatially uniform. Characteristic mean values for the solar wind environment are given in Table 3-2.

Table 3-2: Solar Wind parameters

Parameter	At the Earth (1AU)	Range 5%-95% Limit	
Density (cm^{-3})	8.7	3.0	20
Speed (km s^{-1})	468	320	710
T_p (K)	1.2×10^5	0.098×10^5	3.0×10^5
T_e (K)	1.0×10^5	0.89×10^5	2.0×10^5
T_{alpha} (K)	5.8×10^5	0.60×10^5	15.4×10^5
λ (m)	7.3	-	-
N_{alpha}/N_{proton}	0.047	0.017	0.078

Magnetosheath plasma parameters differ according to the latitude and local time of the observation. The highest density and temperature and the steepest velocity drop are observed at the sub solar point.

3.3 Outer magnetosphere

3.3.1 DESCRIPTION

The magnetosphere is the region of space where the plasma properties are mainly controlled by the Earth's magnetic field. Although the magnetosphere on the day side of the Earth typically only extends to about 10 Earth radii (R_e), it flares out on the flanks and is effectively infinite in length in the anti-solar direction, and it is thus also encountered by the EChO spacecraft in its orbit.

Two distinct plasma regimes can be identified in the magnetosphere around L2 RD[5]: The magnetotail and the magnetosheath. Most of the time in the magnetosphere the EChO spacecraft will be in the magnetosheath, and a smaller fraction of the time in the magnetotail. The ratio depends on the actual orbit. It should be noted that the entire magnetosphere around L2 shows a large variability both in cross-sectional size and orientation due to variations in the solar wind. Also, the solar wind varies on time scales of tens of minutes to days – rapid compared with the orbit of the EChO spacecraft around L2, meaning that within a single orbit the spacecraft is likely to encounter several different plasma regimes.

3.3.2 THE MAGNETOTAIL

Around L2 the magnetotail is approximately cylindrical in shape with a radius of about 20 to 30 R_e. It is an area of relative low density and high energy plasma. The orientation of the magnetotail is determined by the solar wind direction and highly variable. The average aberration angle of the magnetotail from the Sun-Earth line is about 4 degrees (e.g. a shift of the same order as its radius), but can be up to about 10 degrees. This means that the L2 point can be located anywhere in the magnetotail or even in the magnetosheath.

3.3.3 THE MAGNETOSHEATH

The Magnetosheath is surrounding the magnetotail and its outer boundary is the solar wind. Around L2 the radius of the magnetosheath is of the order 100 R_e. It is an area of relative high density and low energy plasma. It should be noted that the orientation is highly variable. The distance from the Sun-Earth line to the outer boundary can vary as much as 75 R_e.

3.3.4 TYPICAL PARAMETERS

Characteristic values for the plasma environment in the magnetotail and the magnetosheath based on Geotail data RD[5] are given in Table 3-3 and Table 3-4 (It is assumed that $T_i=T_{p=}T_{alpha}$ and $N_{alpha}/N_{proton}=0.047$). More information can be found in RD[5] including information on the parameters in the boundary layers.

Table 3-3: Magnetotail parameters (from RD[5]).

Parameter	Average	Range 5%-90% Limit	
Density (cm^{-3})	0.11	0.01	0.35
T_i (K)	63×10^5	9.4×10^5	273×10^5
T_e (K)	21×10^5	7.5×10^5	49×10^5

Table 3-4: Magnetosheath parameters (from RD[5]).

Parameter	Average	Range 5%-90% Limit	
Density (cm^{-3})	1.0	0.28	6.1
T_i (K)	9.3×10^5	1.9×10^5	22×10^5
T_e (K)	3.1×10^5	0.31×10^5	5.6×10^5

3.4 Induced Environments

The natural plasma environment can be augmented by a number of sources inside or on the satellite surface.

High-energy electron and ion populations can be generated by active experiments, i.e. electron and ion guns. These can be used to control surface charging or as a probe of the magnetic field. An ion thruster is a particularly high-flux ion gun.

Low-energy ion populations can be generated by ionisation (including charge exchange) of contaminant gasses i.e. those released from the spacecraft by "outgassing", emitted by thrusters, including ion thrusters and sputtered off the surface due to ion impacts. These contamination processes are described in a separate chapter.

3.4.1 EFFECTS

Once outside the spacecraft, neutral atoms produced by outgassing and sputtering can be ionised by sunlight or charge-exchange with other ions, to create a low-energy (<10eV) ion population. These ions can be drawn to negatively charged surfaces and can adhere. This coating may alter optical properties e.g. of mirrors or solar panel covers, or change the secondary and photoemission yields and the susceptibility to surface charging. Within the spacecraft, e.g. in electronics boxes, residual gasses can facilitate electrostatic discharges from high voltage components.

3.4.2 PHOTO- AND SECONDARY ELECTRONS

The electron density at the spacecraft surface shall be determined from the incident UV and primary electron fluxes, multiplied by the yield for the surface in question. Away from the emitting surface the density shall be calculated from the following formula for a planar surface RD[5]:

$$\frac{N}{N_0} = (1 + \frac{z}{\sqrt{2}\lambda_0})^{-2}$$

where:

N is density (cm^{-3})

N_0 is density at emitter (cm^{-3})

z is distance from surface

λ_0 is shielding distance, calculated as the Debye length due to the emitted electrons

Once neutral gas is released into space by whatever mechanism, it becomes subject to photoionisation and dissociation by solar UV and ionisation by charge exchange with solar wind ions. Production of new ions can be calculated from the appropriate photoionisation rates and charge exchange cross-sections.

$$Q = N_i(\nu + \sigma n_{sw} v_{sw})$$

from RD[7] where:

Q is production rate, ions s^{-1}

N_I is ion density

ν is photoionisation rate coefficient

n_{sw} and v_{sw} are solar wind density and velocity

σ is charge exchange coefficient.

Photoionisation rates depends on the atom or molecule concerned, and UV intensity and spectrum. Huebner and Giguere RD[8] have tabulated a number of rate coefficients for different species, for sunlight at 1AU.

Table 3-5 gives typical photoelectron sheath parameters RD[9].

Table 3-5: Photoelectron Sheath parameters

Parameter	At the Earth (1AU)
Temperature (eV)	3
Photoelectron current (Amps m^{-2})	1×10^{-5}
Surface electron density (m^{-3})	1×10^{8}

4 ENERGETIC PARTICLE RADIATION

4.1 Introduction

In general, the energetic radiation environment consists of magnetically trapped charged particles, solar protons and galactic cosmic rays. It is the penetrating particles that pose the main problems, which include upsets to electronics, payload interference, degradation and damage to components and solar cells, and deep dielectric charging (see also RD[1]). In order to study the effect on the EChO spacecraft the radiation environment need to be assessed. This chapter presents the predicted radiation environment for EChO.

The main components of the radiation environment are:

The Radiation Belts

Energetic electrons and ions are magnetically trapped around the earth forming the radiation belts, also known as the Van Allen belts. The radiation belts are crossed by low altitude orbits as well as high altitude orbits (geostationary and beyond). The radiation belts consist principally of electrons of up to a few MeV energy and protons of up to several hundred MeV energy. The so-called south Atlantic anomaly is the inner edge of the inner radiation belt encountered in low altitude orbits. The offset, tilted geomagnetic field brings the inner belt to its lowest altitudes in the south Atlantic region. More information can be found in references RD[10] and RD[11].

Apart from during the direct escape injection, such radiation belts will not be encountered by the EChO spacecraft during its mission. However the duration is so short that the effect can be ignored.

Solar Particle Events

Events of strongly enhanced fluxes of primarily protons originating from the Sun, usually with a duration on the order of a couple of days. The events occur randomly and mainly during periods of solar maximum. The events are also accompanied by enhanced fluxes of heavy ions. The Earth's magnetic field provides a varying degree of geomagnetic shielding in low Earth orbit.

Galactic Cosmic Rays

A continuous flux of very high energy particle radiation. Although the flux is very low, they include heavy ions capable of causing intense ionisation as they pass through matter. Although their contribution to the total dose is insignificant, they are important when analysing single event effects.

Secondary radiation

Secondary radiation is generated by the interaction of the above environmental components with materials of the spacecraft. A wide variety of secondary radiations are possible, of varying importance.

For EChO by far the main contribution to the radiation dose will be from the solar particle events.

4.1.1 EFFECTS SURVEY

The above radiation environments represent important hazards to space missions. Energetic particles, particularly from the trapped radiation belts and from solar particle events cause radiation damage to electronic components, solar cells and materials. They can easily penetrate typical spacecraft walls and deposit considerable doses during a mission.

Energetic ions, primarily from cosmic rays and solar particle events, lose energy rapidly in materials, mainly through ionization. This energy transfer can disrupt or damage targets such as a memory element, leading to single-event upset (SEU) of a component, or an element of a detector (radiation background).

Energetic particles also interfere with payloads, most notably with detectors on astronomy and observation missions where they produce a "background" signal, which may not be distinguishable from the photon signal being counted, or which can overload the detector system.

Energetic electrons can penetrate thin shields and build up static charge in internal dielectric materials such as cable and other insulation, circuit boards, and on ungrounded metallic parts. These can subsequently discharge, generating electromagnetic interference.

Apart from ionizing dose, particles can lose energy through non-ionizing interactions with materials, particularly through "displacement damage", or "bulk damage", where atoms are displaced from their original sites. This can alter the electrical, mechanical or optical properties of materials and is an important damage mechanism for electro-optical components (solar cells, opto-couplers, etc.) and for detectors, such as CCDs.

4.2 Quantification of effects and related environments

Models of the radiation environment are needed to assist in orbit selection, component selection and shielding optimization. In engineering a space system to operate in the space environment, it is necessary to relate the environment to system degradation quantitatively. This also involves questions of testing systems and their components for verification that they meet the performance requirements in the presence of the space environment.

For example, testing with calibrated radioactive sources can establish the threshold for functional failure or degradation of an electronic component in terms of *total absorbed dose*. Radiation environment models, used together with mission orbital specifications can predict the dose and enable correct performance to be verified.

Table 4-1 below gives the parameters which shall be used for quantification of the various radiation effects.

Although some of these parameters are readily derivable from a specification of the environment, others either need explicit consideration of test data (for example single-event upset calculation) or

the detailed consideration of interaction geometry and mechanisms (e.g. radiation background estimation).

Table 4-1: Parameters for quantification of radiation effects

	Parameter
Electronic component degradation	Total ionizing dose.
Material degradation	"
Material degradation (bulk damage)	Non-ionizing dose (NIEL).
CCD, sensor and opto-electronic component degradation	NIEL
Solar cell degradation	NIEL & *equivalent fluence.*
Single-event upset, latch-up, etc.	LET spectra (ions); proton energy spectra; explicit SEU/SEL rate of devices.
Sensor interference (background signals)	Flux above above energy threshold and/or flux threshold; explicit background rate.
Internal electrostatic charging	Electron flux and fluence; dielectric E-field.

In the following sections, the basic data on the environment are presented, along with models to be employed for deriving data beyond those presented. Effects and the specific methods for derivation of engineering quantities will then be presented. Figure 4-1 shows the ranges of electrons and protons in aluminium.

4.3 Reference data models and analysis methods

4.3.1 TRAPPED RADIATION BELTS MODELS

These are not applicable for the interplanetary orbit of the EChO spacecraft, but are only mentioned here for completeness.

For trapped radiation, the standard models of radiation belt energetic particle shall be the AE-8 and AP-8 models for electrons RD[12] and protons RD[13] respectively. They were developed at the NSSDC at NASA/GSFC based on data from satellites flown in the '60s and early '70s. The models give omni-directional fluxes as functions of idealized geomagnetic dipole co-ordinates B/B_0 and L. This means that they must be used together with an orbit generator and geomagnetic field computation to give instantaneous or orbit-averaged fluxes. The user must define an orbit, generate a trajectory, transform it to geomagnetic co-ordinates and access the radiation belt models to compute flux spectra. Apart from separate versions for solar maximum and solar minimum, there is no description of the temporal behaviour of fluxes and no explicit flux directionality. For more information including information about which field model to use see RD[1].

4.3.2 SOLAR PARTICLE EVENT MODEL

During energetic events on the sun, large fluxes of energetic protons are produced which can reach the Earth. Solar particle events, because of their unpredictability and large variability in magnitude, duration and spectral characteristics, have to be treated statistically. However, large events are confined to a 7-year period defined as solar maximum. Although large events are absent during the remaining 4 solar minimum years of the 11-year solar cycle the occasional small event can still occur. The model used for engineering consideration of time-integrated effects is the ESP model RD[14]. This statistical model is based on data from 3 solar cycles and gives the proton fluences at 1AU and it has superseded the JPL-91 RD[15], which was previously the standard. To give a worst case the entire mission is assumed to take place during solar maximum conditions. The confidence level applied in the solar proton calculation is 90%. Figure 4-2 and Figure 4-3 shows the predicted spectrum for the EChO mission of solar protons based on this model both as plot and in tabular form.

The individual flare spectra are very variable, and what constitutes a worst-case event for a given energy is not necessarily worst-case at another. For the higher energies, which are the most important for nuclear interactions giving rise to certain types of background and single-event upsets, the October 1989 event is normally seen as a worst-case. This event produced a fluence of about 2.2 10^{10} protons.cm^{-2} with energies above 10 MeV (with a peak flux of 10^5 protons.cm^{-2}.s^{-1} with energies above 10 MeV).

Concerning the directionality of the event flux, there is a streaming taking place, but it is usually of short duration (short compared with the duration of the individual event), with field disturbances quickly changing it into near isotropic distribution. Also it seems less pronounced in larger events. Therefore for the design the flux can be assumed to be isotropic. More information can be found in RD[16].

Near the Earth, the magnetic field partially shields the space from solar energetic particles and cosmic rays. However the L2 orbit is too far away from the Earth for this to a significant effect for EChO.

Individual Solar particle events

While the ESP model provides data only for integrated effects analysis (dose, long-term degradation, total upset count, etc.), it is often necessary to consider individual events. Burrell, as reported in RD[17], developed a modified Poisson statistic to describe the probability p of a number of events n occurring during a time t, based on a previously observed frequency of N during time T:

$$p(n,t;\, N,T) = \{(n+N)!\ (t/T)^n\} \,/\, \{n!N!\ (1+t/T)^{N+n+1}\}$$

In this equation, N=1 and T=7 for the anomalous class of flare, while for ordinary flares, N=24 and T=7. This is sometimes useful in considering numbers of events in contrast to the total fluence.

Often it is necessary to consider instantaneous fluxes. For radiation background estimation for example, the fluxes are required above an energy threshold determined by sensor shielding and sensor sensitivity, and above a flux threshold determined by sensor signal-to-noise characteristics. Two reference environment data resources are available: NASA OMNIWEB database RD[18], and

the NOAA GOES RD[19] database. With these databases, the durations and magnitudes of events above energy and flux thresholds can be analysed. Both databases are available on the WWW and provide a comprehensive long-term database of measurements of the interplanetary environment. OMNIWEB contains a complete database of energetic proton data from the IMP series of spacecraft. The NOAA GOES satellites have returned energetic proton and electron data from geostationary orbit since January 1986.

Solar particle event ions

For analysing single event upset rates during solar particle events (SPE's), the CREME96 model shall be used. It can also be used for other applications where data on severe SPE conditions are needed, such as background estimation. CREME96 is described further in RD[20]. While the older CREME model contained models for the peak flux for various types of events, CREME96 contains models based on the October 1989 event. It provides models of energy spectrum, composition and LET spectrum for the worst week, worst day and peak 5 minutes. The older CREME model provided more choice of peak environments. However, some of the more severe options were unrealistic.

4.3.3 COSMIC RAY ENVIRONMENT AND EFFECTS MODELS

To assess Single Events Effects (SEE) the Linear Energy Transfer (LET, dE/dx) spectrum is needed. To assess this the CREME96 software RD[20] is used. CREME96 is the standard model for cosmic ray environment assessment and provide a comprehensive set of cosmic ray and flare ion LET and energy spectra, including treatment of geomagnetic shielding and material shielding. It also included upset rate computation based on the path-length distribution in a sensitive volume and also treated in a simple manner trapped proton-induced SEUs. It is used for evaluation of single event effects from cosmic rays, from solar energetic particles and from energetic protons. Cosmic ray fluxes are anti-correlated with solar activity so the highest cosmic ray fluxes occur at solar minimum.

Figure 4-4 and Figure 4-5 show the results from a calculation of the LET using the CREME96 software in respectively graphical and tabular form. The prediction is assuming a shielding of $1 g/cm^2$ (equivalent to about 3.7mm Aluminium). The predicted LET spectrum is given for the peak 5 minutes of a solar particle event (representing a worst case), for the worst week and the background galactic cosmic ray LET spectrum (this is the predicted continuous background galactic cosmic ray flux).

4.3.4 SPACECRAFT SECONDARY RADIATION

For engineering purposes it is often only electron-induced Bremsstrahlung radiation that is considered as a significant secondary source. Bremsstrahlung is high-energy electromagnetic radiation in the X-γ energy range emitted by charged particles slowing down by scattering off atomic nuclei. The primary particle might ultimately be absorbed while the Bremsstrahlung can be highly penetrating. In space, the most common source of Bremsstrahlung is electron scattering. In special cases other secondaries need to be considered.

In evaluating the radiation background effects in detector systems, it is often secondary radiation that is important. This might be because of heavy shielding removing primaries, veto systems which actively protect against counting primary-induced signals, or secondary radiation generated within the sensing band of an instrument. Most secondary radiation is emitted at the instant of interaction ("prompt") while some is emitted some time after a nucleus has been excited by an incoming particle (induced radioactivity).

By its nature, secondary radiation has to be analysed on a case-by-case basis, possibly through Monte-Carlo simulation. For engineering estimates of Bremsstrahlung, the SHIELDOSE model RD[21] shall be used.

Neutrons

Neutrons are generated by energetic particles undergoing nuclear interactions with the material of spacecraft. These neutrons play a role in generating background in sensitive detector systems. A low-level flux of neutrons of between 0.5 $cm^{-2}.s^{-1}$ and 4 $cm^{-2}.s^{-1}$ is also present at low altitudes around the Earth due to cosmic ray interactions with the atmosphere.

4.4 Analysis methods for derived quantities

The following analysis methods shall be used.

The environment models specified in 4.3 shall be used to generate the primary data described in 4.2. The secondary data shall be derived as follows:

4.4.1 IONIZING DOSE

The ionizing dose environment is traditionally represented by the dose-depth curve. This may provide dose as a function of shield thickness in planar geometry or as a function of spherical shielding about a point. The planar model is appropriate for surface materials or for locations near to a planar surface. In general, electronic components are not in such locations and a spherical model is recommended for general specification.

SHIELDOSE is the general model used RD[21] for ionizing dose. This method uses a pre-computed data set of doses from electrons, electron-induced Bremsstrahlung and protons, as derived from Monte-Carlo analysis. The doses are provided as functions of material shielding thickness. The reference geometrical configuration for this dose-depth curve shall be a solid aluminium sphere. Figure 4-6 and Figure 4-7 shows the corresponding ionising doses as calculated by the SHIELDOSE software as implemented in SPENVIS RD[2]. The figures show the total ionising radiation dose in Si as a function of spherical aluminium shielding thickness. The dose is completely dominated by the contribution from solar electrons. The accumulated dose of solar energetic protons are shown in the figures with a confidence level of 90% that higher dose will not be seen. It should be remarked that no specific radiation design margin is included in the presented figures. The doses presented are for equivalent aluminium shielding.

The main analysis methods to assess the detailed radiation effect on a spacecraft are:

- Sectoring analysis
- Particle transport simulation

The sectoring analysis is the simplest and quickest, but it implies a number of simplifications:

- Separation of the environment and the spacecraft
- Merging of all particles types and all energies
- Merging of all materials and all configurations
- Particle propagation in straight lines (i.e. lack or treatment of radiation scattering and secondary production)

Therefore for a more detailed and more accurate analysis it is recommended to perform a full particle transport simulation (e.g. applying tools like GEANT4 RD[22]).

Sectoring Analysis

In cases where more careful analysis of the shielding of a component or of other sensitive locations is necessary, a sectoring calculation is performed on the geometry of the system. This might be necessary if the doses computed from simple spherical shielding are incompatible with the specification of the allowable radiation dose. The sectoring analysis calculates the radiation doses in a 3D geometry model, by performing a "sectoring" of the actual shielding. The sectoring method traces rays from the point of interest through the shielding in a large number of directions. Along each direction the derived shielding, together with the data on dose as a function of shielding depth, d, is used to find the omni directional 4π dose contribution from each direction. The contributions, weighted by the solid angle increment around the rays, are then summed to give the total dose. The analysis relies on a separation of the environment and the model of the spacecraft. The environment is represented by a dose depth curve giving the total dose as a function of shielding thickness for a certain reference material usually aluminium.

In some cases, it is efficient to derive a shielding distribution. This is the result of the ray tracing described above and provides the distribution of encountered shielding. To this distribution the shielding of the unit under investigation itself must be added and it can then be folded with the dose depth curve to derive the total dose.

It is important to recognise that a shielding analysis in the presence of significant anisotropies in the environment can result in serious error if the environment is assumed to be isotropic. This assumption is implicit in the sectoring method defined above since all directional contributions are derived from a common "omni directional" dose-depth curve.

Particle Transport Simulation

For the particle transport simulation the GEANT4 family of tools tool can be used. GEANT4 RD[22] is an open source object-oriented toolkit for the simulation of particle transport in matter. It is developed, maintained and still continuously upgraded by a large international collaboration. While initially focussed on High Energy Physics (HEP) experiments, it is currently used also in domains such as nuclear physics, astrophysics and space science, medical physics and nuclear medicine, radio-protection.

GEANT4 offers a wide set of electromagnetic and hadronic physics models, a good performance of the particle transport in complex geometry models and the possibility of interfacing to external packages such as simulation engines and visualization or analysis tools. The level of accuracy of the physics processes, and their wide range of applicability in terms of particle types, energy range and target material description make GEANT4 well suited for any energetic particle environment and its interaction with a spacecraft.
The GEANT4 Radiation Analysis for Space (GRAS) RD[23] is a GEANT4-based tool that performs common radiation analyses (including TID, NIEL, fluence, path length, charge deposit and dose equivalent, etc) from Monte Carlo transport in generic 3D geometry models. GRAS can be used for obtaining a variety of simulation output types for whichever (GDML or C++) 3D geometry model. This avoids the creation of a new tailored C++ GEANT4-based application for every new project. Thanks to a modular design, the GRAS analysis type capabilities are being easily extended. Space radiation sources range from very low to very high energy, and their interactions with the spacecraft sensitive devices and the shielding structures include both electromagnetic and hadronic processes. The GRAS tool includes therefore a very large subset of the physics models available within GEANT4, with the aim of giving an almost complete coverage of the main interaction mechanisms for trapped, solar and cosmic radiation in the spacecraft materials. The geometry models from the MULASSIS tool RD[22] (multi-layered planar or spherical configurations) are available from GRAS.
GEANT4 can also be used for simple sectoring analysis via its Sector Shielding Analysis Tool (SSAT), which performs ray-tracing from a user-defined point within a geometry to determine shielding levels (the fraction of solid angle for which the shielding is within a defined interval), shielding distribution (the mean shielding level as a function of look direction) and total TID- or NIEL-doses. To achieve this, the tool (based on the GEANT4 particle transport toolkit) utilises the fictitious geantino particle, which undergoes no physical interactions, but flags boundary crossings along its trajectory. Ray-tracing options include SLANT, NORM and WEIGHTED modes. Knowledge of the positions of these boundary crossings together with the density of the material through which the particle has passed can be used to profile the shielding (in g/cm^2, cm, or radiation lengths) for a given point within the geometry. The shielding information can be used, together with a user-provided external dose-depth curve, to determine the total dose at a point.

Shielding Optimisation

It is also important to recognise that some materials are better at stopping particular forms of radiation than others. While heavier materials can be efficient at stopping electrons, lighter materials are usually more efficient at stopping protons. This can not be analysed with the SHIELDOSE model. To assess the relative shielding effectiveness of different materials the MULASSIS tool RD[22], which is based on the Geant4 simulation toolkit RD[22], can be used.

With these tools different shielding materials can be investigated in order to find the most effective shielding at the lowest mass. The best shielding depends on the particles species and energies. As a general remark, for protons the use of low Z materials is the best option, while for electrons best shielding can be achieved by interleaving materials with different densities (from low to high Z) in a sandwich configuration.

4.4.2 SINGLE-EVENT UPSET RATE

The CREME/CREME96 method shall be used RD[20]. It is possible to make upset rate predictions only when details of the device under consideration are known, particularly the critical charge and the sensitive volume dimensions. If a device is uncharacterised, tests shall be performed.

The test data shall show the normalised upset rate as a function of ion LET in the range 1 to 100 MeV·cm^2/mg and as a function of proton energy in the range 20-100MeV. These data shall be used to make an estimate of the upset rate from trapped protons and solar protons using the two-parameter Bendel method RD[25], and of upsets due to galactic and solar ions using the method of CREME/CREME96. This latter shall be modified to account for the non-ideal upset rate as a function of ion LET derived from component test data RD[26] (the so-called "IRPP" method) as described below. This method has been implemented in CREME96. CREME96 also includes the two-parameter Bendel method.

To compute an upset rate for an electronic device or a detector from the predicted fluxes, device characteristics must be specified, particularly the size of the sensitive volume and the *critical charge*, or equivalently, critical energy E_c, in the volume which results in upset or registers as a "count". For SEUs resulting from direct ionisation the rate is found by integrating over the composite differential ion LET spectrum and the distribution of path-lengths for the sensitive volume RD[26],RD[27]. An estimate of the upset rate from nuclear interactions of energetic protons can be obtained by integration of the product of the measured proton-induced upset cross section $\sigma(E)$ and the differential proton flux $f(E)$ over all energies. $\sigma(E)$ can be derived directly from the test data, or the 2-parameter Bendel fit can be used.

4.4.3 SOLAR CELL DEGRADATION

For assessment of degradation to solar cells a dedicated version of the EQFRUX code available in SPENVIS RD[2] is used. In the absence of other test data, it is assumed that 10MeV protons cause equivalent damage to 1000 1 MeV electrons for maximum power in gallium arsenide cells. Infinite rear-side shielding of cells is assumed. Figure 4-8, Figure 4-9 shows the resulting predicted equivalent 1MeV electron fluences for solar cell degradation for the different phases of the EChO mission as functions of the cover glass thickness.

4.4.4 INTERNAL ELECTROSTATIC CHARGING

Internal electrostatic charging (or deep-dielectric charging) results from the build-up over a longer period of electrostatic charge. The charge build-up depends on the severity of the environment and the dielectric resistivity of the susceptible part (or lack of grounding of floating metalisation). The actual discharge may also depend on properties such as geometry and material condition. Charge build-up can therefore be mitigated by choice of material and grounding, but also by employing shielding to reduce the severity of the environment.

Tools are available to address these issues, such as DICTAT, which has been incorporated SPENVIS RD[2]. More complex tools are also available like ESADDC RD[28], which employs a Monte-Carlo radiation transport method to compute the charge build-up in a dielectric material in a certain environment.

4.4.5 NON-IONIZING DOSE

Damage to CCDs and other electro-optical components susceptible to displacement damage shall employ the NIEL function (non-ionising energy loss), N(E) RD[29], to derive a 10MeV equivalent proton damage fluence F_D:

$$F_D = \Sigma_E f(E) \cdot N_{10}(E) \cdot \Delta E$$

or a non-ionizing dose, D_N:

$$D_N = \Sigma_E f(E) \cdot N(E) \cdot \Delta E$$

where: $f(E)$ is the differential fluence spectrum

$N(E)$ is the NIEL function

$N_{10}(E)$ is the NIEL function normalised to 10MeV

ΔE is the energy step of the sum.

Figure 4-10 shows the NIEL function for protons and Silicon as target material.

Figure 4-11 shows the non ionising energy loss for the EChO mission. To turn this into a relative degradation (e.g. Charge Transfer Efficiency loss in a CCD) it is necessary to test the specific detector in question to find its response to such an environment. Traditionally the equivalent 10MeV proton fluence is quoted. Often it is necessary to test with higher energies than 10MeV, for instance due to the required penetration depth, therefore the equivalent 60Mev and 200MeV equivalent proton damage fluences are also included in Figure 4-12.

The NIEL is strongly dependent on the particle type and to a lesser extent on the target material. Heavier ions causes far more damage per nucleon for the same particle energy than lighter ones.

4.5 Links with radiation testing

The Table 4-2 below recalls the parameter used for quantification of various radiation effects, and for illustration purposes, lists the types of testing which must be done to verify compatibility with the effects.

Table 4-2: Links with radiation testing

Radiation effect	Parameter	Test means
Electronic component degradation	Total ionising dose	Radioactive sources (e.g ^{60}Co), particle beams (e^-,p^+)
Material degradation	Total ionising dose	Radioactive sources (e.g ^{60}Co), particle beams (e^-,p^+)
Material degradation (bulk damage)	Non-ionising dose (NIEL)	Proton beams
CCD and sensor degradation	Non-ionising dose (NIEL)	Proton beams
Solar cell degradation	Non-ionising dose (NIEL) & *equivalent fluence.*	Proton beams (~ low energy)
Single-event upset, Latch-up,etc.	LET spectra (ions), proton energy spectra, explicit SEU/L rate.	Heavy ion particle beams Proton particle beams ⇦
Sensor interference (background signals)	Flux above energy threshold, flux threshold, explicit background rate.	Radioactive sources, particle beams ⇦
Internal electrostatic Charging	Electron flux and fluence dielectric E-field.	Electron beams ⇦ Discharge characterisation

⇦ = test data feed back to calculation

e, p = electron, protons

4.6 Figures

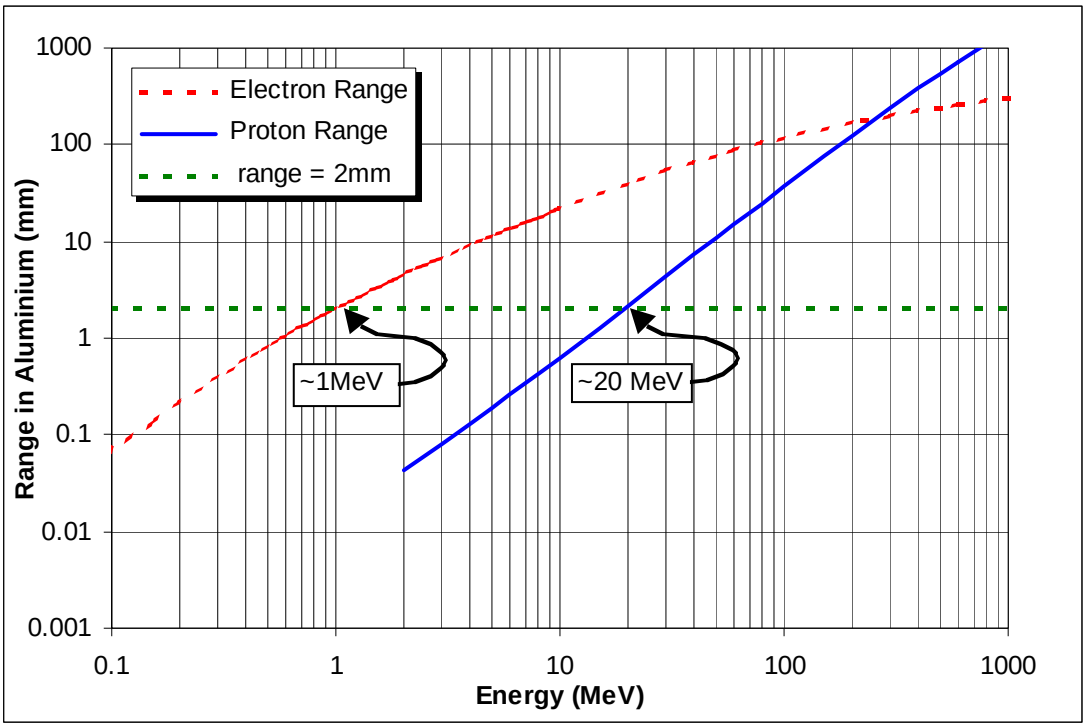

Figure 4-1: Mean ranges of protons and electrons in aluminium

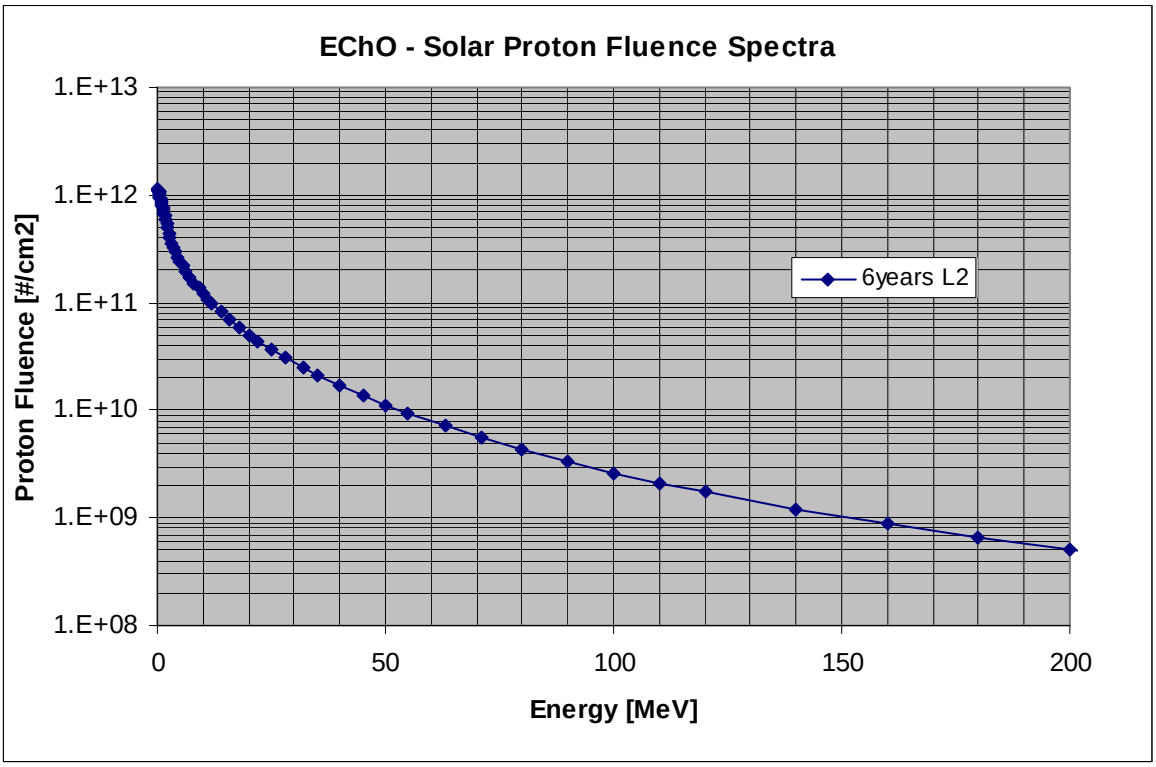

Figure 4-2: Integral Solar Proton Fluence for the EChO Mission

Energy [MeV]	Integral Fluence [/cm2]
	Extended mission (6 years)
0.1	1.15E+12
0.2	1.11E+12
0.5	9.84E+11
1	8.08E+11
1.6	6.37E+11
2	5.44E+11
2.5	4.46E+11
3.2	3.51E+11
4	2.96E+11
5	2.39E+11
6.3	1.95E+11
8	1.54E+11
10	1.20E+11
12	9.90E+10
16	6.88E+10
20	5.06E+10
25	3.66E+10
32	2.49E+10
40	1.70E+10
50	1.13E+10
63	7.18E+09
80	4.32E+09
100	2.61E+09
120	1.74E+09
160	8.73E+08
200	4.98E+08
250	2.79E+08
320	1.39E+08
400	6.44E+07
500	2.46E+07

Figure 4-3: Integral Solar Proton Fluence for the EChO Mission

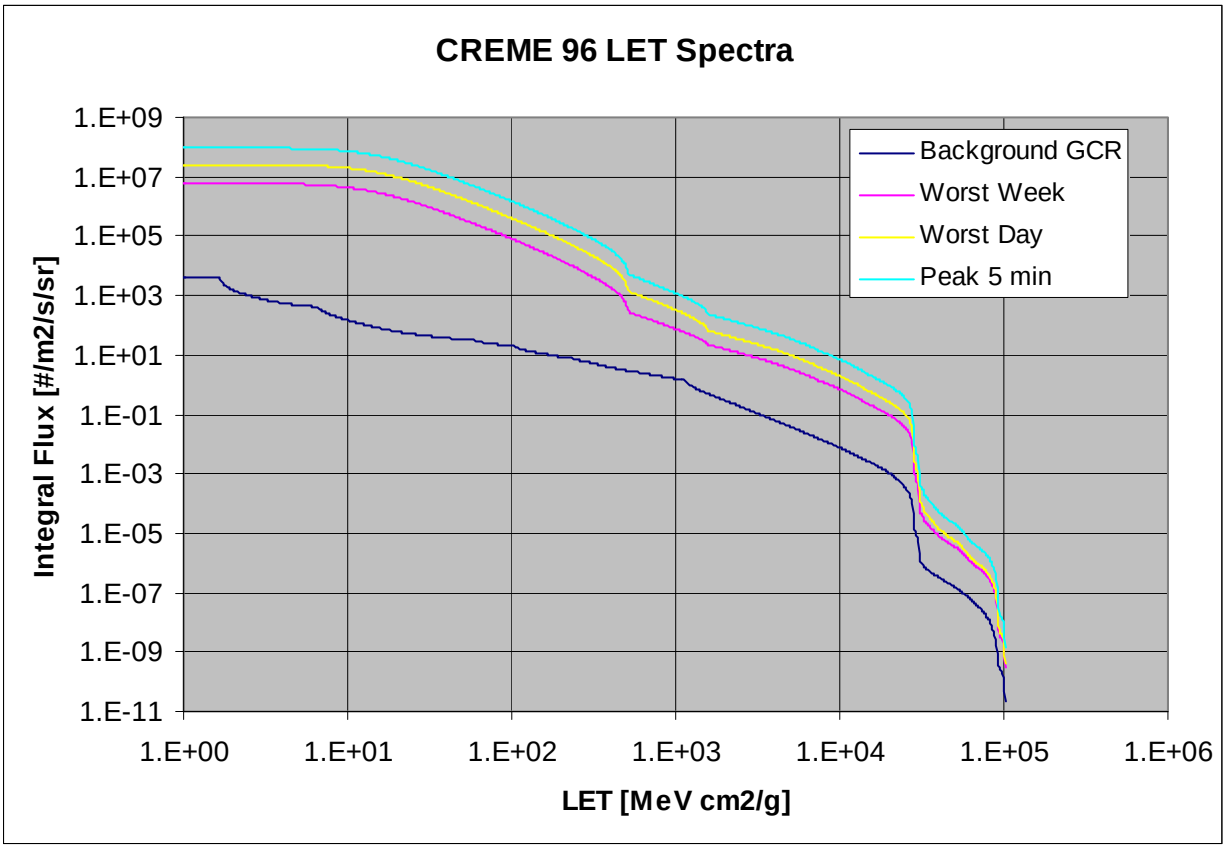

Figure 4-4: CREME96 Galactic Cosmic Ray LET Spectra for the three levels of activity, nominal (quiet), worst week, and peak 5 minute (worst case) for a component shielded by 1 g/cm^2.

LET [MeV cm2/g]	Integral GCR Flux [#/m2/sec/sr]		
	Quiet	Worst Week	Peak 5 Min
1.00E+00	3.90E+03	5.94E+06	9.24E+07
1.35E+00	3.90E+03	5.94E+06	9.24E+07
1.83E+00	2.02E+03	5.94E+06	9.24E+07
2.47E+00	1.01E+03	5.92E+06	9.23E+07
3.34E+00	6.68E+02	5.87E+06	9.18E+07
4.52E+00	5.07E+02	5.72E+06	9.04E+07
6.11E+00	4.29E+02	5.41E+06	8.69E+07
8.25E+00	2.06E+02	4.84E+06	7.97E+07
1.12E+01	1.26E+02	3.99E+06	6.76E+07
1.51E+01	8.43E+01	2.96E+06	5.15E+07
2.04E+01	6.03E+01	1.97E+06	3.50E+07
2.76E+01	4.69E+01	1.20E+06	2.15E+07
3.73E+01	3.92E+01	6.77E+05	1.23E+07
5.04E+01	3.34E+01	3.66E+05	6.70E+06
6.81E+01	2.60E+01	1.92E+05	3.53E+06
9.21E+01	2.08E+01	9.83E+04	1.82E+06
1.25E+02	1.39E+01	4.90E+04	9.08E+05
1.68E+02	1.03E+01	2.37E+04	4.40E+05
2.28E+02	7.84E+00	1.07E+04	1.99E+05
3.08E+02	5.49E+00	4.50E+03	8.38E+04
4.16E+02	3.69E+00	1.61E+03	2.99E+04
5.62E+02	2.70E+00	2.34E+02	4.29E+03
7.60E+02	2.04E+00	1.31E+02	2.26E+03
1.03E+03	1.54E+00	7.13E+01	1.13E+03
1.39E+03	6.71E-01	3.58E+01	4.91E+02
1.88E+03	3.34E-01	1.73E+01	1.82E+02
2.54E+03	1.74E-01	1.11E+01	1.15E+02
3.43E+03	9.01E-02	6.86E+00	7.09E+01
4.64E+03	4.58E-02	3.97E+00	4.13E+01
6.27E+03	2.28E-02	2.11E+00	2.18E+01
8.48E+03	1.12E-02	1.03E+00	1.05E+01
1.15E+04	5.41E-03	4.98E-01	5.00E+00
1.55E+04	2.36E-03	2.04E-01	2.01E+00
2.10E+04	8.91E-04	8.10E-02	7.98E-01
2.83E+04	1.28E-05	1.00E-03	9.46E-03
3.83E+04	3.83E-07	1.04E-05	6.99E-05
5.18E+04	1.37E-07	3.09E-06	1.80E-05
7.00E+04	3.42E-08	6.80E-07	3.41E-06
9.46E+04	2.76E-10	3.73E-09	1.81E-08
1.10E+05	0.00E+00	0.00E+00	0.00E+00

Figure 4-5: CREME96 Galactic Cosmic Ray LET Spectra for the three levels of activity, nominal (quiet), worst week, and peak 5 minute (worst case) for a component shielded by 1 g/cm^2..

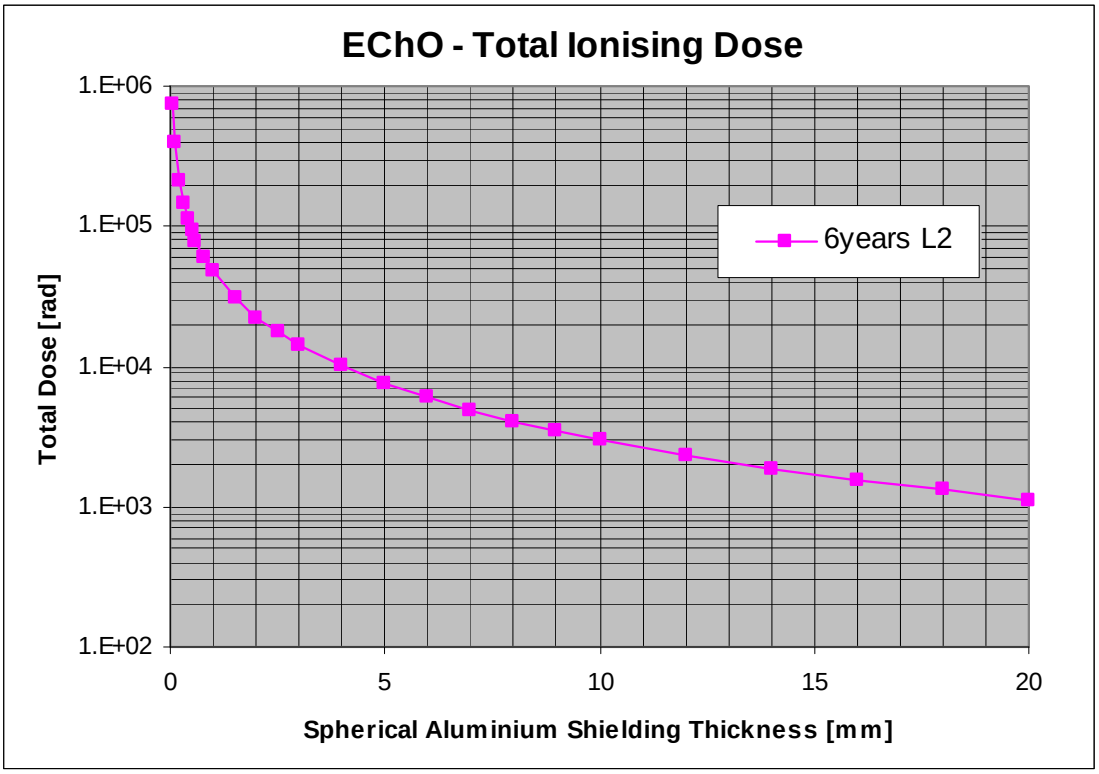

Figure 4-6: Dose in Si as a function of spherical Al shielding as calculated by SHIELDOSE

Shielding Thickness [mm]	Total ionising dose in Si for Spherical Al Shielding Extended mission (6 years)
0.05	7.56E+05
0.1	3.93E+05
0.2	2.10E+05
0.3	1.48E+05
0.4	1.14E+05
0.5	9.34E+04
0.6	7.77E+04
0.8	5.91E+04
1	4.80E+04
1.5	3.14E+04
2	2.25E+04
2.5	1.75E+04
3	1.42E+04
4	1.00E+04
5	7.56E+03
6	6.04E+03
7	4.91E+03
8	4.10E+03
9	3.52E+03
10	3.02E+03
12	2.35E+03
14	1.88E+03
16	1.55E+03
18	1.31E+03
20	1.11E+03

Figure 4-7: Total Ionising dose in Si for Spherical Al Shielding as calculated by SHIELDOSE

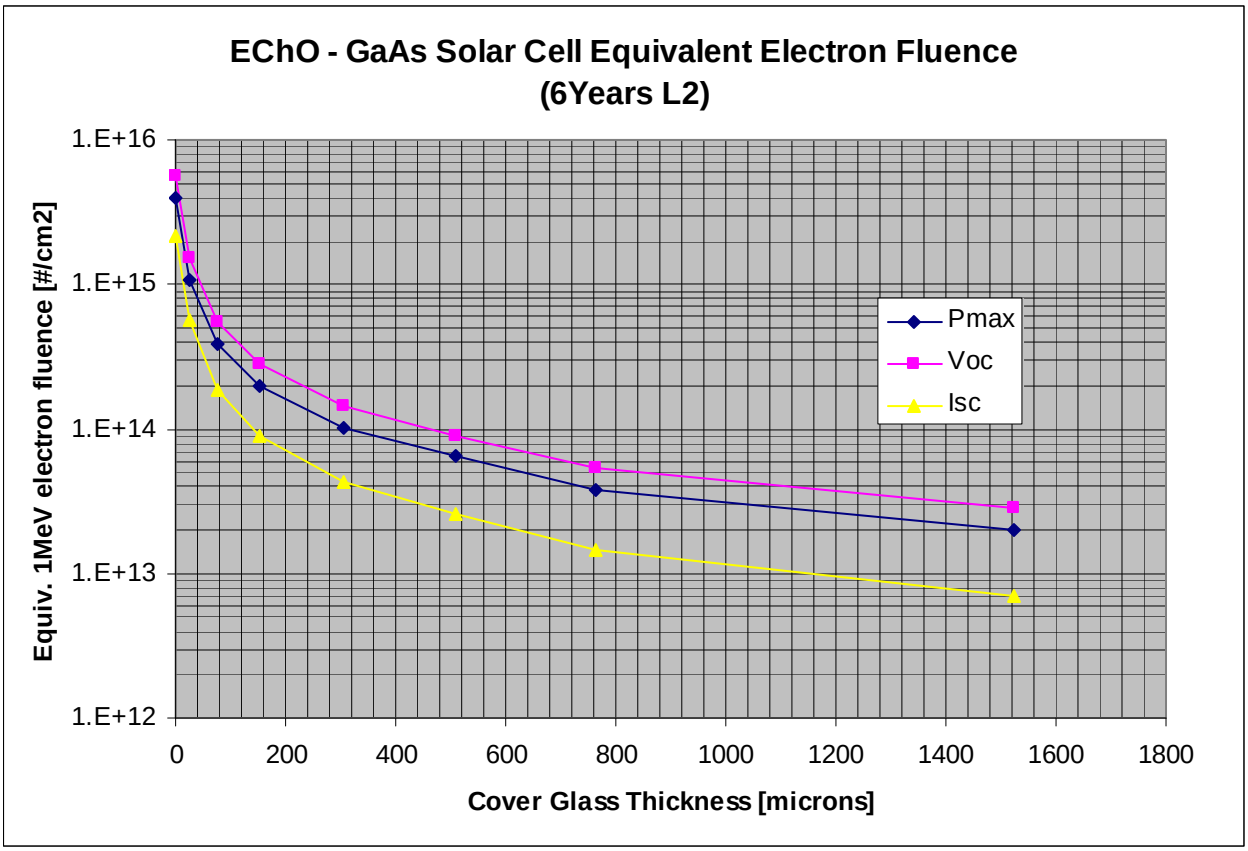

Figure 4-8: Equivalent 1MeV electrons for Pmax for GaAs solar cells degradation

Solar cells equivalent 1MeV electron fluence for GaAs cells (Electron/proton damage ratios: Pmax: 1000.0, Voc: 1400.0, Isc: 400.0) (Coverglass: material: fused silica, density: 2.20 g/cm3)				
Cover Glass Thickness		Total		
[g/cm2]	[Microns]	Pmax [#/cm2]	Voc [#/cm2]	Isc [#/cm2]
0	0	3.99E+15	5.58E+15	2.17E+15
0.0056	25.4	1.09E+15	1.52E+15	5.64E+14
0.0168	76.2	3.88E+14	5.43E+14	1.87E+14
0.0335	152.4	1.99E+14	2.79E+14	8.99E+13
0.0671	304.8	1.02E+14	1.43E+14	4.34E+13
0.1118	508	6.42E+13	8.98E+13	2.61E+13
0.1676	762	3.83E+13	5.37E+13	1.45E+13
0.3353	1524	2.00E+13	2.81E+13	6.94E+12

Figure 4-9: Equivalent 1MeV electrons for GaAs solar cells degradation for EChO extended mission (6years l2)

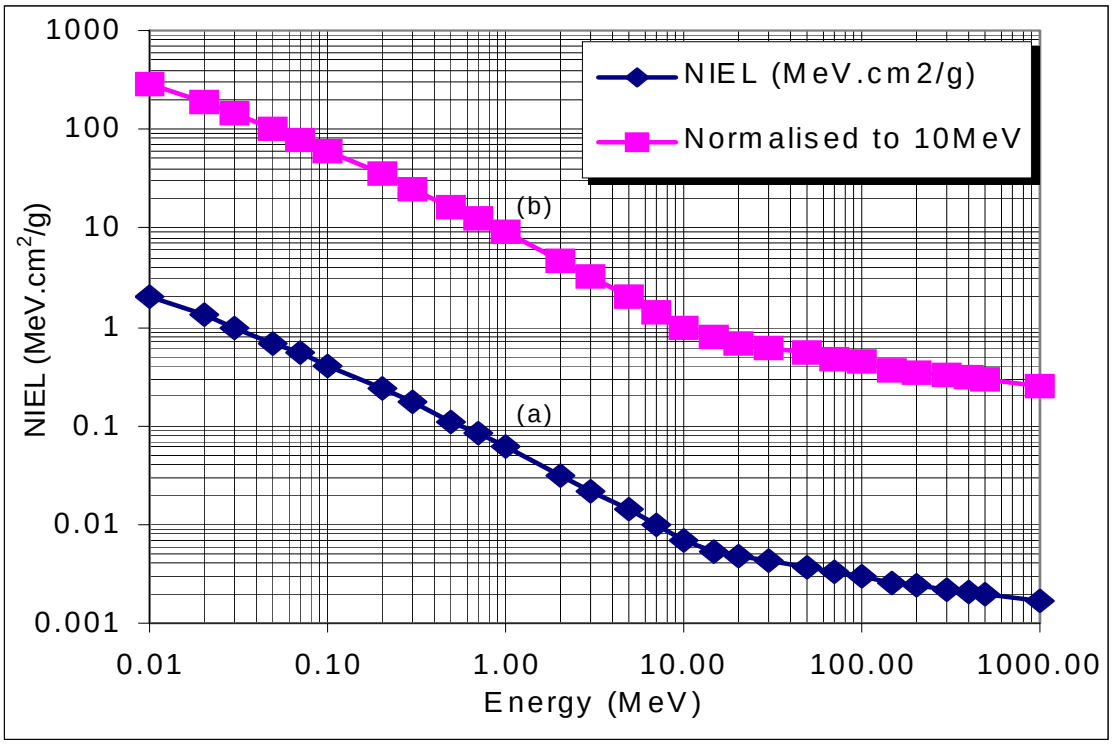

Figure 4-10: NIEL curve: (a) energy lost by protons in non-ionizing interactions (bulk, displacement damage); (b) NIEL relative to 10MeV giving damage-equivalence of other energies

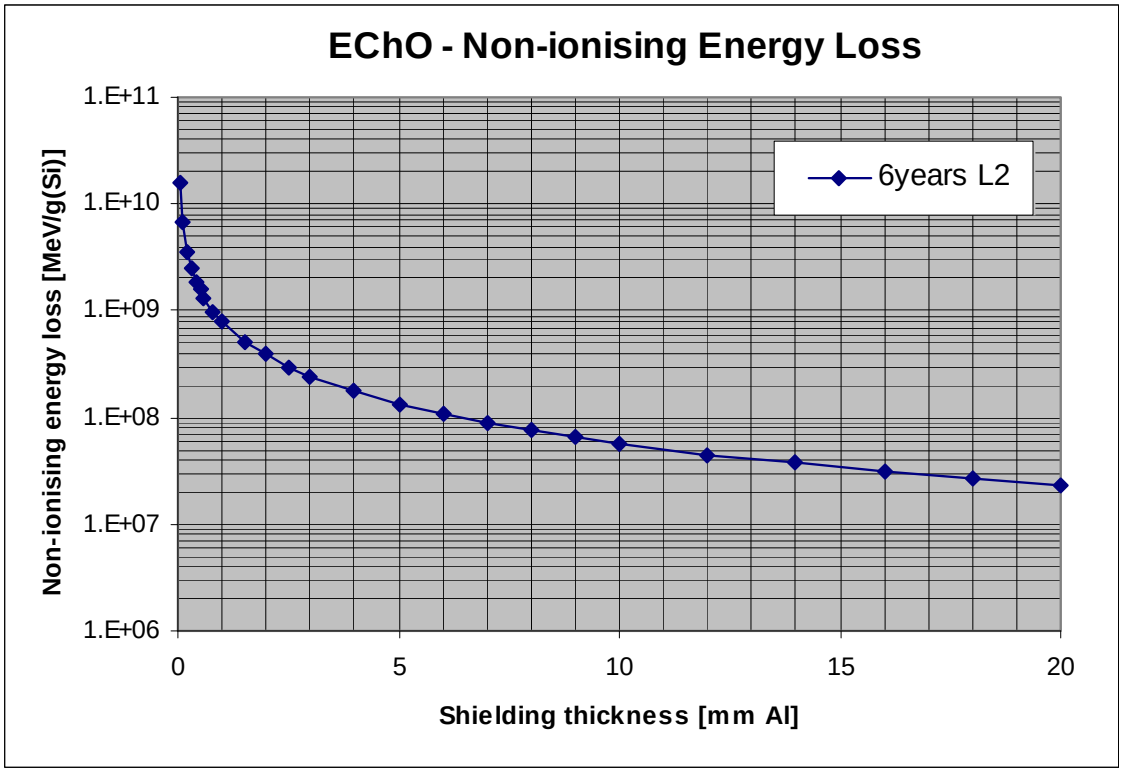

Figure 4-11: Non-Ionising Energy Loss as a function of shielding thickness for the EChO mission

Aluminium shielding thickness [mm]	Non ionising energy loss and equivalent proton fluence			
	Energy loss [MeV/g(Si)]	Eq 10MeV Proton fluence [#/cm2]	Eq 60MeV Proton fluence [#/cm2]	Eq 200MeV Proton fluence [#/cm2]
0.05	1.58E+10	2.29E+12	4.56E+12	6.58E+12
0.1	6.95E+09	1.01E+12	2.01E+12	2.90E+12
0.2	3.55E+09	5.14E+11	1.03E+12	1.48E+12
0.3	2.56E+09	3.71E+11	7.41E+11	1.07E+12
0.4	1.89E+09	2.74E+11	5.48E+11	7.89E+11
0.5	1.57E+09	2.28E+11	4.55E+11	6.55E+11
0.6	1.32E+09	1.92E+11	3.82E+11	5.51E+11
0.8	9.77E+08	1.42E+11	2.83E+11	4.07E+11
1	7.96E+08	1.15E+11	2.30E+11	3.32E+11
1.5	5.08E+08	7.36E+10	1.47E+11	2.12E+11
2	3.90E+08	5.66E+10	1.13E+11	1.63E+11
2.5	2.96E+08	4.29E+10	8.55E+10	1.23E+11
3	2.46E+08	3.57E+10	7.12E+10	1.03E+11
4	1.74E+08	2.52E+10	5.03E+10	7.25E+10
5	1.34E+08	1.94E+10	3.86E+10	5.57E+10
6	1.08E+08	1.57E+10	3.14E+10	4.52E+10
7	9.06E+07	1.31E+10	2.62E+10	3.78E+10
8	7.53E+07	1.09E+10	2.18E+10	3.14E+10
9	6.58E+07	9.54E+09	1.90E+10	2.74E+10
10	5.78E+07	8.38E+09	1.67E+10	2.41E+10
12	4.52E+07	6.55E+09	1.31E+10	1.88E+10
14	3.72E+07	5.39E+09	1.08E+10	1.55E+10
16	3.10E+07	4.49E+09	8.97E+09	1.29E+10
18	2.66E+07	3.86E+09	7.70E+09	1.11E+10
20	2.27E+07	3.29E+09	6.57E+09	9.47E+09

Figure 4-12: Non-Ionising Energy Loss and equivalent proton fluences as a function of shielding thickness for the EChO extended mission (6years L2)

5 PARTICULATES

5.1 Introduction

Every spacecraft in orbit is exposed to a certain flux of micrometeoroids. Spacecraft in Earth orbit encounter man-made space debris as well. Collisions with these particles will take place with hypervelocity speed (typically 10 to 20km/s).

Meteoroids are particles of natural origin. Nearly all meteoroids originate from asteroids or comets. The natural meteoroid flux represents, at any instant, a total of about 200 kg of mass within 2000 km of the Earth's surfaceRD[30]. Meteoroids that retain the orbit of their parent body can create periods of high flux and are called streams. Random fluxes with no apparent pattern are called sporadic.

Space debris is man-made. Space debris particles are mainly encountered in earth orbits below 2000 km altitudes and near the geostationary ring.

The damage caused by collisions with meteoroids and space debris will depend on the size, density, speed and direction of the impacting particle and on the shielding of the spacecraft. Submillimeter sized particles can cause pitting and cratering of outer surfaces and lead to degradation of optical, electrical, thermal, sealing or other properties. Larger particles can puncture outer surfaces and may cause damage to structure or equipment by penetration and spallation.

Flux models have been developed for both micrometeoroids and space debris. The resulting damage can be assessed through empirically derived design equations which give penetration capabilities, crater sizes, etc. as function of the particle parameters and target properties.

As the EChO spacecraft will spend only very limited time near Earth impacts from space debris particles can be neglected and in the following impacts from meteoroids only will be considered.

5.2 Analysis techniques

Meteoroid impacts are specified by statistical flux models. Meteoroid fluxes are usually specified as a time-averaged flux, F_r, to one side of a randomly tumbling surface. Flux is defined as number of intercepted objects per unit time and area. The relevant area for F_r is the actual outer surface area of a spacecraft element.

For spacecraft which fly with a fixed orientation, the directionality of the meteoroid fluxes should be taken into account. Most impacts from meteoroids will occur on forward facing surfaces.

The number of impacts, N, increases linearly with exposed area and with exposure time:

$$N = F \times A \times T$$

where F is the number of impacts per unit area, A is the total exposed area and T is the exposure time.

Fluence is the flux integrated over time.

Once N has been determined, the probability of exactly n impacts occurring in the corresponding time interval is given by Poisson statistics:

$$P_n = (N^n)/n!) \; . \; e^{-N}$$

The probability for no impacts, P_0 is thus given by:

$$P_0 = e^{-N}$$

For values of $N << 1$ the probability, Q, for at least one impact ($Q = 1 - P_0$) is equal to N:

$$Q = 1 - e^{-N} \approx 1 - (1 - N) = N$$

All these equations apply as well if the number of impacts, N, is replaced by the number of failures, NF, resulting from an impact.

5.3 Meteoroid model presentation

For meteoroids, the isotropic flux model given in RD[31] shall be used. This model gives the total average meteoroid **flux** (sporadic + stream average) in terms of the integral flux $F_{met,0}$ which is the number of particles with mass m or larger per m^2 per year impacting a randomly-oriented flat plate under a viewing angle of 2π . The unshielded interplanetary flux at 1 AU distance from the sun is according to the model described by the analytical formula:

$$F_{met,0}(m) = 3.15576\times10^7(F_1(m) + F_2(m) + F_3(m))$$

where:

$$F_1(m) = (2.2\times10^3 \; m^{0.306} + 15)^{-4.38}$$

$$F_2(m) = 1.3\times10^{-9}(m + 10^{11} \; m^2 + 10^{27} \; m^4)^{-0.36}$$

$$F_3(m) = 1.3\times10^{-16}(m + 10^6 \; m^2)^{-0.85}$$

with m in grams.

Meteoroid **velocities** near Earth can range from 11 to 72 km/s. The velocity distribution with respect to Earth to be used with the isotropic reference flux model given in RD[31] is (number per km/s):

	0.112	if $11.1 \le v < 16.3$ km/s
$g(v) =$	$3.328\times10^5 \; v^{-5.34}$	if $16.3 \le v < 55.0$ km/s
	1.695×10^{-4}	if $55.0 \le v < 72.2$ km/s

The average velocity of this distribution is close to 17 km/s.

The unshielded flux $Fmet_{,0}$ has to be modified to account for the **gravitational attraction** (which enhances the meteoroid flux in the Earth proximity) and the geometrical shielding of the Earth (which reduces the flux). The gravitational enhancement factor G_e is according to RD[30]:

$$G_e = 1 + R_E / r$$

where

R_E is the mean Earth radius
r is the orbit radius

For the EChO trajectory the earth gravitational attraction can be ignored (Ge =1).

The Earth shielding factor, s_f, for a given surface depends on the altitude and on the relative orientation of the surface normal with respect to the Earth direction (according to RD[1]). For the EChO trajectory the earth shielding can be ignored (s=1).
The meteoroid flux to an Earth orbiting spacecraft is then given by:

$$F_{met} = F_{met,0} \times G_e \times s_f$$

The mass density of meteoroids varies widely from about 0.15 g/cm^3 to 8 g/cm^3.

For the directional distribution the annual averaged meteoroid flux is usually considered to be omnidirectional with respect to the Earth surface. Relative to a spacecraft with fixed orientation with respect to the flight direction the meteoroid flux has a directional dependence, introduced by the motion of the spacecraft together with the Earth shielding effect. The directional dependence of meteoroids has then to be calculated numerically by converting the omnidirectional flux to the flux on a specific surface with given surface orientation and spacecraft velocity vector.
The meteoroid flux model described above gives a yearly average. Meteoroid streams are accumulations of meteoroids with nearly identical heliocentric orbits. Relative to Earth all particles of a given meteoroid stream have nearly identical impact directions and velocities. Encounters with meteoroid streams typically lasts from a few hours to several days.
At peak activity stream fluxes can exceed the sporadic background fluxes by a factor 5 or more. Occasionally, very high fluxes (meteoroid storms, the visible meteor background flux can be exceeded by a factor 10000 or more) can be encountered for short periods (1-2 hours).
Meteoroid streams are believed to consist of relative large particles only (mass > 10^{-8} - 10^{-6} g) with low density (0.5-1.0 g/cm^3).

Tailoring guidelines

Values for average mass densities of meteoroids are:

Low: 1.0 g/cm^3

Nominal: 2.5 g/cm^3

High: 4.0 g/cm^3

For analysis of effects the nominal value of 2.5 g/cm^3 shall be used.
For the assessment of impact effects the full velocity distribution and the full directional impact distribution of meteoroids should be used.

For a preliminary analysis a constant meteoroid impact velocity of 20 km/s and an impact angle of 45º (from the surface normal) shall be used.
A spherical shape shall be assumed to convert particle masses and diameters.
For EChO the yearly averaged model can be used.

5.4 Reference data

Cumulative meteoroid and space debris fluxes (i.e. fluxes of particles of given size or larger) can be obtained directly from the flux models. Figure 5-1 gives the number of impacts /m^2 from one side to a randomly oriented plate for a range of minimum particle sizes. The results are for the 1AU. The meteoroid fluxes are from the model given in 34. For meteoroids a density of $\rho = 2.5$ g/cm^3 and the assumption of spherical shape were used to convert masses to diameters. The MASTER-2005 model RD[32] was used for the debris fluxes. Figure 5-2 gives the same data in tabulated form.

Meteoroids directionality

The present meteoroid flux model assumes an isotropic flux with respect to the Earth surface. For an orbiting spacecraft the Earth shielding and the spacecraft motion both introduce a directional dependence. The Earth shielding factor is given in 5.3. The directionality caused by the spacecraft motion leads to increased fluxes on forward facing surfaces and to reduced fluxes on trailing surfaces. Combining the two factors the following flux ratios for meteoroids are found for the EChO trajectory (using the velocity distribution from 5.3):

front/random	≈1.5
front/rear	≈ 2.5
space face/Earth face	≈1.05

As resulting effects like penetration depth or impact plasma generation also depend on parameters like impact velocity and angle, the directional ratios for these effects can be considerably different from those given above.

5.5 Model uncertainties

The meteoroid environment flux models given above contain several known approximations and other uncertainties.
According to RD[30] uncertainties in the meteoroid models mainly result from uncertainties in particle densities and masses. Fluxes for meteoroids larger than 10^{-6} g are well defined, but the associated masses are quite uncertain. The mass density of meteoroids spans a wide range, from about 0.15 g/cm^3 to values as large as 8 g/cm^3. At a set mass this implies an uncertainty in the flux

of a factor 0.1 to 10. For meteoroids smaller than 10^{-6} g flux uncertainties at a given mass are estimated to be a factor of 0.33 to 3.

5.6 Damage assessment

In this section a brief general overview of damage assessment criteria and procedures is given. For each individual project the damage assessment has to be tailored according to the specific conditions and requirements (e.g. shielding, damage criteria, required reliability, etc.). Any damage assessment depends to a large extent on the relevant failure criteria. Possible failure criteria include:

- cratering (sensor degradation, window blinding, surface erosion)
- larger craters (sealing problems, short circuits on solar arrays)
- impact generated plasma (interference, discharge triggering)
- wall penetration (damage, injury, loss of liquid or air)
- burst, rupture (pressurised parts)
- structural damage

For a quantitative damage and risk assessment, so-called damage or design equations for the given shielding configuration are needed. They give shielding thresholds or hole sizes for given impacting particle parameters and failure mode. One of the most widely used damage equation gives the threshold thickness for penetration of single metal plates (thin plate formula):

$$t = k_m \, m^{0.352} \, \rho^{0.167} v^{0.875}$$

where:

t:	threshold thickness for penetration [cm]
km:	material constant, 0.55 for Aluminium
m:	mass of projectile [g]
ρ:	density of projectile [g/cm^3]
v:	normal impact velocity component of projectile [km/s]

A puncture occurs whenever the threshold thickness for an impacting particle with given mass, density and velocity exceeds the shielding thickness of the surface under consideration. Finding a realistic damage equation for a given shielding configuration can be problematic. The translation of a failure mode to a damage equation can be difficult. Many damage equations for different types of shields and for different velocity regimes have been developed. However, for most materials, compounds, and shielding concepts no specific damage equation is available.
Sometimes scaled effective thickness in combination with known damage equations can be used for a first assessment. For impact damage and risk assessments secondary ejecta should be considered as well. Every hypervelocity impact leads to the ejection of secondary particles which can impact other surfaces (depending on the spacecraft geometry). The total mass of the ejected particles can exceed the mass of the primary impactor by orders of magnitude. Secondary particles

will be typically ejected within a cone around the impact direction. Their velocities are typically below 2 km/s. At present, quantitative models of secondary ejecta are not mature enough to be used as standard.

5.7 Analysis tools

Several numerical tools have been developed to perform impact and impact risk analyses. One possible tool is the ESABASE/DEBRIS RD[33]. It is a statistical tool and was developed for a detailed impact risk assessment of smaller, non-trackable particles. ESABASE/DEBRIS is a fully three dimensional numerical analysis tool including directional and geometrical effects and spacecraft shielding considerations. It is based on environment and particle/wall interaction models and includes the reference meteoroid and space debris flux models defined in this document. The user specifies the mission, spacecraft geometry, attitude and shielding as well as the particle type, size and velocity range to be analysed. The computed output includes:

- the number of impacts,
- the resulting number of damaging impacts taking into account the spacecraft shielding and damage assessment equations,
- the mean particle impact velocity (amplitude and direction),
- the numbers of craters of specified size,
- the probability of no failure.

5.8 Figures

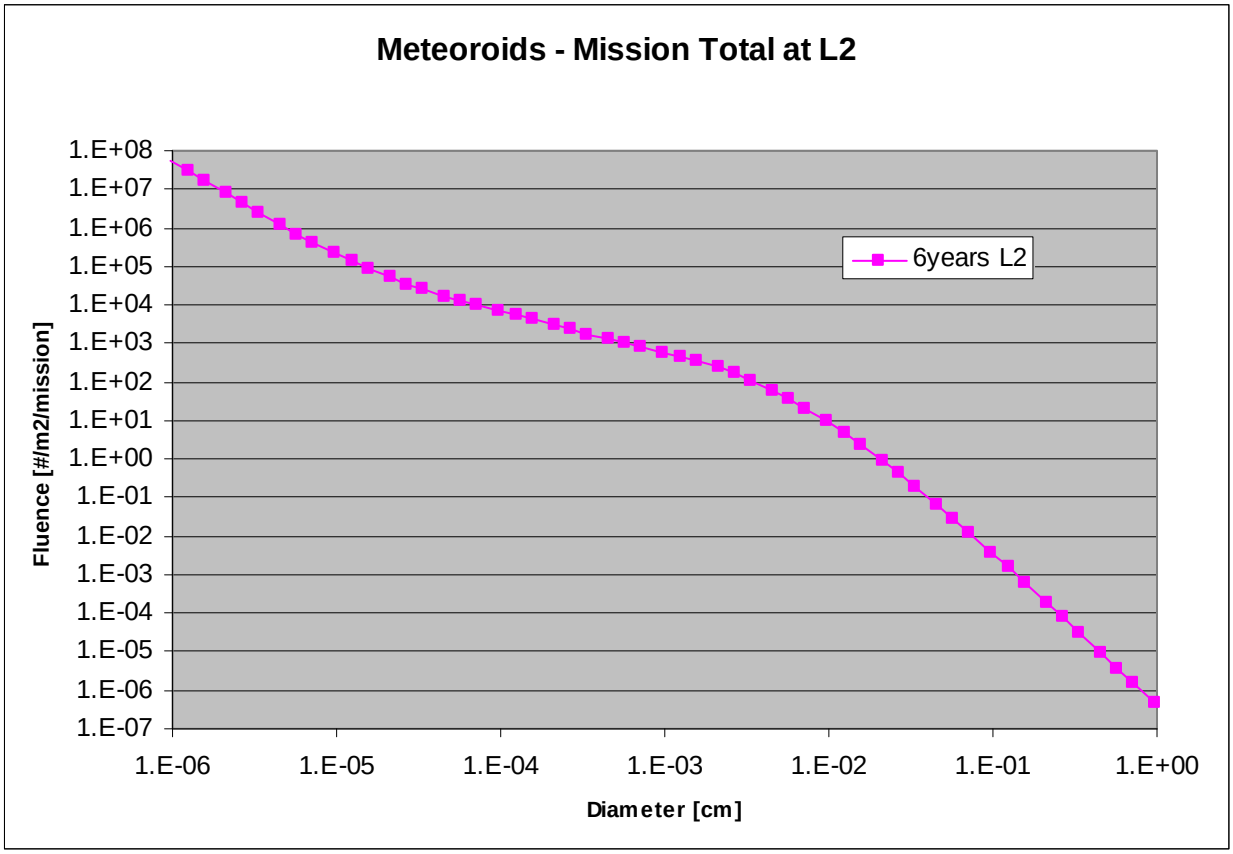

Figure 5-1: Cumulative number of impacts, N, to a randomly oriented plate for a range of minimum particle sizes. The results are for interplanetary at 1AU. The meteoroid fluxes were obtained by the model from Gruen et al

Mass, m [g]	Diameter, D [cm (ρ = 2 g/cm^3)]	Fluence, N [/m^2 /year]
1.00E-18	9.85E-07	8.80E+06
1.00E-17	2.12E-06	1.28E+06
1.00E-16	4.57E-06	1.98E+05
1.00E-15	9.85E-06	3.56E+04
1.00E-14	2.12E-05	8.44E+03
1.00E-13	4.57E-05	2.78E+03
1.00E-12	9.85E-05	1.15E+03
1.00E-11	2.12E-04	4.99E+02
1.00E-10	4.57E-04	2.14E+02
1.00E-09	9.85E-04	1.01E+02
1.00E-08	2.12E-03	3.96E+01
1.00E-07	4.57E-03	1.01E+01
1.00E-06	9.85E-03	1.58E+00
1.00E-05	2.12E-02	1.55E-01
1.00E-04	4.57E-02	1.10E-02
1.00E-03	9.85E-02	6.32E-04
1.00E-02	2.12E-01	3.26E-05
1.00E-01	4.57E-01	1.58E-06
1.00E+00	9.85E-01	7.44E-08

Figure 5-2: Cumulative number of impacts, N, to a randomly oriented plate for a range of minimum particle sizes. The results are for interplanetary at 1AU. The meteoroid fluxes were obtained by the model from Gruen et al

6 CONTAMINATION

6.1 Introduction

This chapter deals with the induced molecular and particulate (solid or liquid) environment in the vicinity of and created by the presence of the EChO spacecraft in its orbit. It is meant mainly to aid in the definition of the contamination environment (foreign or unwanted matter that can affect or degrade the performance of any component when being in line of sight with that component or when residing onto that component). The relevant computer models and tools are also presented.
The quantitative modelling of the contamination environment is very complex. This is due to the high number of materials involved, with a variability of outgassing characteristics. Furthermore, there are interactions of the outgassing products with surfaces, residual gas and with other environmental parameters such as solar radiation, atomic oxygen.
The contamination analysis, which necessarily is very much dependent of a specific application, cannot be more detailed in this specification. ECSS-Q-ST-70-01C RD[34] defines amongst others the requirements to be followed and guidelines to be taken into account in order to control the particulate and molecular contamination within the specified limits during a mission.

It is the responsibility of the user:

- to estimate the sensitivity of his system/equipment with regard to contamination
- to identify the contamination sources on his experiment
- to evaluate with all appropriate means the expected contamination levels/quantities present in critical areas, taking into account the mechanisms of transport and fixation of contaminants.

6.2 Molecular contamination

6.2.1 SOURCES OF MOLECULAR CONTAMINATION

6.2.1.1 Outgassing of Organic Materials

Outgassing of organic materials can be approached as a surface evaporation combined with a diffusion for bulk contaminant species. These species can be either initially present components, or decomposition products.
Initially present outgassing species can be: water, solvents, additives, uncured monomeric material, lubricants, ground contamination species, due to e.g. processes, test, storage, handling, pre-launch and launch.
The decomposition products are due to exposure of molecular materials to other environments, such as: thermal, solar radiation, electromagnetic and charged particles, atomic oxygen , impacts by micrometeoroids or debris, electrical discharges and arcing

These products consist of lower molecular weight (higher volatility) species than the original species.

6.2.1.2 Plumes

Plume species can result from combustion, unburned propellant vapours, incomplete combustion products, sputtered material and other degradation products from a propulsion or attitude control system and its surroundings swept along with the jet.
Plumes can also be produced by dumps of gaseous and liquid waste materials of the environment control and life support systems in manned spacecraft or by leaks in systems or internal payloads.
Contamination of surfaces not in direct view is possible due to ambient scattering (collisions with other residual atmosphere species), self scattering (collisions with other identical or different contaminant species) or ionisation of the molecules under radiation, e.g. UV or particles, and subsequent attraction to a charged surface.

6.2.1.3 Pyrotechnics and release mechanisms

During operation of pyrotechnics or other release mechanisms gases can evolve.

6.2.1.4 Secondary sources

A surface can act as a secondary source if an incoming contaminant molecule will reflect (not accommodate stick or condense on the surface) or if it has a limited residence time on that surface. Secondary sources can for example be solar panels having a higher temperature than the surrounding surfaces.

6.2.2 TRANSPORT MECHANISMS

Apart from the direct flux there are different transport mechanisms by which a contaminant molecule can reach a surface. Surface accommodation occurs when a molecule becomes attached to a surface long enough to come into a thermal equilibrium with that surface (an accommodation coefficient can be defined as a measure for the amount of energy transfer between the contaminant molecule and the surface). It is useful to define the concept of a sticking coefficient as the probability that a molecule, colliding with a surface, will stay onto that surface for a time long compared to the phenomena under investigation. The sticking coefficient is a function of such parameters as contamination/surface material pairing, temperature, photo-polymerisation, reactive interaction with atomic oxygen.

6.2.2.1 Reflection on surface

A molecule will reflect on a surface when the accommodation coefficient during a collision is zero, i.e. when there is no energy transfer between the molecule and the surface during that collision. A reflection of a molecule is always specular, although this will be dependent on surface roughness, RMS).

6.2.2.2 Re-evaporation from surface

A molecule having a non-zero residence time can re-evaporate from a surface. Re-evaporation is diffuse, i.e. the molecule is leaving the surface following a Lambertian distribution law.

6.2.2.3 Migration on surface

A molecule accommodated on a surface can migrate over that surface.

6.2.2.4 Collision with residual (natural) atmosphere

The contamination environment shall take into account the collision between the contamination species and the residual atmosphere. This interaction results in an ambient scattering of the contamination species, and can sometimes lead to an increase in the local pressure.

6.2.2.5 Collision with other outgassed molecules

The contamination environment shall take into account the collision between two contamination molecules. This interaction results in self-scattering of the contamination species.

6.2.2.6 Ionisation by other environmental parameters

A molecule can be ionised due to interaction with (V)UV or charged particles (electrons, protons, ions) and subsequently be attracted by a charged surface.

6.2.2.7 Permanent Molecular Deposition (PMD)

Molecular matter can permanently stick onto a surface (non-volatile under the given circumstances) as a result of reaction with surface material, UV-irradiation or residual atmosphere induced reactions (e.g. polymerisation, formation of inorganic oxides).

6.3 Particulate contamination

6.3.1 SOURCES OF PARTICULATE CONTAMINATION

Sources inherent to materials: particles originating from manufacturing (machining, sawing), handling (e.g. for brittle materials such as certain paints) or wear (friction); degradation of binder under different environments (e.g. AO, UV...) resulting in loose filler; crack formation and subsequent flaking as a result of thermal cycling; formation of particles due to oxidation in an Atomic Oxygen environment.
Sources external to materials: dust particles can be caused by atmospheric fall-out (dust) during assembly, integration and storage or by human sources during such activities (hair, skin flakes, lints or fibres from garments...); particles can be produced during spacecraft propulsion or attitude control operations, the functioning of moving parts (such as shutters), and water dumps; particles can result from micrometeoroid or debris impacts on materials.

6.3.2 TRANSPORT MECHANISMS

Particles can be transported by vibrations due to launch, (attitude control) manoeuvring and docking. Pyrotechnic shocks can cause particles to migrate from one surface to another.
Particles can be charged due to their interaction with ambient plasma or photo emission, and subsequently attracted by electrically charged surfaces.
For specific missions other mechanisms can have an effect on the particles, such as: drag, due to the residual atmosphere in the lowest Earth orbits; radiation pressure due to solar radiation; gravitational tide, e.g. re-attraction to spacecraft.

6.4 Effect of contamination

The primary concerns of contamination are related to the degradation of spacecraft elements or sub-system performances due to the presence of:

- deposited species onto a critical surface:

  (thermo-)optical properties, such as transmission, reflection, absorption, scattering, tribological properties, outgassing of lubricant, friction due to particles electrical properties, such as surface conductivity, secondary emission and photo-emission.

- glow or other surface/gas reactions
- free flying species in the field of view of sensors:

  light scattering (star trackers)
  light absorption
  background increase (natural environment analysis)

The effect of a contamination can be altered by the exposure to other environmental parameters, e.g. UV can increase the absorption due to photo-degradation (darkening) of the deposited contaminant, Atomic Oxygen can have a cleaning-up effect on hydrocarbon material, but can also form non-volatile SiOx that can further trap other contaminants.

6.5 Models

Worst case outgassing modelling can be based on screening thermal vacuum test (VCM-test) to determine the outgassing properties of materials. The test is described in ECSS-Q-ST-70-01C RD[34] and ASTM-E595 RD[36]. The test results are:

TML -- Total Mass Loss (sum of condensable and non-condensable material), measured ex-situ as a difference of mass before and after exposure to a vacuum under the conditions specified in the outgassing test.

RML -- Recovered Mass Loss (difference between the initial mass and the mass after re-climatisation after the vacuum test, showing the amount on non-water products in the total mass loss).

CVCM -- Collected Volatile Condensable Material (Low Vapour Pressure, condensable material), measured ex-situ on a collector plate after exposure (to a vacuum) under the conditions specified in the outgassing test.

TML, RML and CVCM are normally expressed in % of the initial mass of the material.
More sophisticated outgassing/condensation models will take into account the data of outgassing or mass flow rates, surface accommodation and sticking coefficients as obtained by e.g. the ECSS-Q-ST-70-02C RD[37] or the ASTM E-1559 test RD[38].

6.5.1 OUTGASSING SOURCES

For a material that outgassses at a constant rate, independently of the quantity present, such as e.g. during evaporation or sublimation from a bulk, the process can be described as a zero order reaction.

$$dm/dt = k$$

with:

dm/dt	outgassing rate in $g \cdot cm^{-2} \cdot s^{-1}$
k	reaction constant

The weight-loss through evaporation, at a temperature T is given by RD[39]

$$dm/dt = 0.04375 \cdot P_s \cdot (M/T)^{1/2}$$

with:

P_s	Vapour Pressure in mbar
dm/dt	weight-loss per unit area in $g \cdot cm^{-2} \cdot s^{-1}$
M	Molecular mass
T	Temperature in K

The outgassing is often described as a first order reaction RD[40], i.e. the material outgasses at a rate that is proportional to the mass available, and using Arrhenius law for the temperature dependency. Important parameters for the outgassing rate are temperature, exposed surface area (or the surface available for evaporation), surface morphology, dimensions of the material (characteristic dimension, thickness).

$$dm/dt = - m/\tau$$

with τ being a temperature dependent time constant of the outgassing phenomenon. Integration gives:

$$m = m_0 \cdot \exp(-t/\tau)$$

Assuming the Arrhenius relation to be valid

$$\tau = \tau_0 \exp(-E/RT)$$

it is possible to determine the outgassing as function of temperature.

The mass loss can be expressed as

$$m_{loss} = m_o \cdot m = m_o \cdot (1 - \exp(-t/\tau)$$

6.5.1.1 Plumes

Evaluation of plumes of thrusters or vents is often described by specific application related models. Parametric descriptions of plumes constitute an interesting alternative to spacecraft designers.
The mass flux Φ of a plume can be expressed in the most generic form

$$\Phi (r, \Theta) = f(r, \Theta, dm/dt)$$

with

$\Phi(r, \Theta)$ flux at a given position from the vent

r radial distance from the vent

Θ angle from the centerline of the vent

dm/dt Mass flow from the vent

where moreover the function f will depend on the plume type. However this formula can in general be reduced in a good approximation to the product

$$\Phi (r, \Theta) = A \cdot (dm/dt) \cdot f_l(\Theta) \cdot r^{-2}$$

where A is a normalisation coefficient.

For a thruster, the function f_l is peaked around $\Theta=0$ and can be expressed as a sum of decreasing exponentials RD[41] or as a (high) power law of $\cos(\Theta)$ or both RD[42]. It is in some extent specific of each thruster.

Plumes from vents are more standard and the f_l function can consequently be fixed: the mass flux is approximated by the following engineering model

$$\Phi (r, \Theta)=((n+1)/(2 \pi)) \cdot (dm/dt) \cdot \cos^n(\Theta) \cdot r^{-2}$$

where $1 \leq n \leq 2$ are typical values used for design. The divergence is larger than the one of thrusters.

6.5.2 TRANSPORT OF MOLECULAR CONTAMINANTS

6.5.2.1 Transport between surfaces

This section only deals with the methods and models for transport of neutral molecules. There is no available model of ion transport devoted to contamination.
Three levels of complexity and accuracy in modelling the transport of neutral molecular contaminants can be distinguished.

6.5.2.2 Simplest view factors

This model simulates collisionless transport. In such a case the fraction of contaminants coming from surface j to surface i is given by the view factor Vij of surface i seen from surface j (including the cosine factor coming from lambertian emission law). These view factors are similar to the ones of radiative thermal analysis. They can be computed geometrically or by Monte-Carlo ray tracing. The incident mass on a surface i is then given by

$$S_j \, V_{ij} \cdot dm_j/dt$$

where j runs over all surfaces and dm_j/dt denotes the outgassing mass rate of surface j.

6.5.2.3 Simplified Monte-Carlo

Collisions of contaminants are simulated in a simplified way, the density and speed of possible partners for molecular collisions are given a priori:

- for ambient scatter, the ambient density and speed are easily known, but wakes (or 'shades') are usually not treated,
- for self-scatter, the contaminant density is very simplified and usually taken proportional to $1/r^2$ and with spherical symmetry.

This method is usually limited to one collision per molecule because the uncertainties due to the densities given a priori increase with collision number. This effective view factors can conveniently be computed by Monte-Carlo ray-tracing method.
Both methods can include other contaminant sources such as vents and plumes. The view factors are then replaced by interception factors.

6.5.2.4 True Monte-Carlo (Direct Simulation Monte-Carlo DSMC)

This computes multiple collisions in a realistic way. The collision probabilities are computed auto-coherently from the densities given by the simulation. This method is far more time consuming and requires more work for programming (in particular it requires a meshing of volume and not only of spacecraft surfaces).
Either method can be better suited, depending on the spacecraft configuration. A potential contamination of a sensitive protected surface through multiple collisions shall require a precise DSMC simulation. In simpler cases, when contamination essentially happens in line-of-sight, it shall be more appropriate to use the less time-consuming methods.

6.5.2.5 Surface transport

Reflections on surfaces and re-evaporation are easy to implement and are usually included in models, the latter (re-evaporation) often as part of the outgassing process. Migrations on surfaces on the contrary are complex processes and there is no commercial available model.

6.5.2.6 Transport of particles

As mentioned earlier particulate transport is governed by several phenomena:

- atmospheric drag
- solar radiation pressure
- differential gravitational effects (with respect to spacecraft) which result in tide effects
- particulate charging and subsequent electrostatic effects

Among which the first three may be computed by methods similar to spacecraft orbit computing, whereas point 4 requires specific modelling to assess particulate charging in a plasma and potential map around spacecraft. The dominant phenomena are most commonly modelled: point 1, atmospheric drag, first, and also point 4 that gets important in GEO. Points 2 and 3 may become dominant in cases when points 1 and 4 become small (high altitude and no charging).
A last aspect of particulate transport is their interaction with walls. Sticking and accommodation coefficients are however very difficult to assess.
Most particulate contamination models remain in the field of research. Very few of them seem to be transferable to other users.

6.6 Specific Requirements

The external contamination requirements are based on the criticality of the mission, i.e. the sensitivity of systems (thermal blankets, solar arrays, radiators, star trackers etc.) as well as payload (optical sensors, cameras, spectrometers etc.) to contamination.
Generally the user shall:

- Perform an assessment of the system or equipment contamination sensitivity;
- Identify the contamination sources on-board;
- Evaluate, in accordance with ECSS-Q-ST-70-01C, the expected contamination levels or quantities present in critical areas, assessing the mechanisms of transport and fixation of contaminants.
- Define the modelling requirements and where quantitative levels are required use a physical outgassing and contamination transport model.

Some tentative overall external contamination requirements for the EChO spacecraft can be derived from previous specifications for other projects like the external contamination control requirements for the Soho. The requirements shall be such that the deposition of organic contaminants will not exceed the following level (integrated over the entire mission):

- Total molecular deposition of 30 Ångstrøm per year (this correspond to some 10^{-6}g/cm^2 or about 300ng/cm^2/year).

The requirement is intended to be achievable at minimum cost if considered early in the design, and reflect the maximum level that can be tolerated. Within the overall limit, the various spacecraft elements can be assigned contamination allocations not to be exceeded. It is important for each element not to exceed the limit in order not to cause unacceptable degradation of the overall spacecraft thermal control and power production performance. Payloads (or the proximity of such)

with e.g. cryogenic (or relatively cold sensitive surfaces) or optics (UV, visible) can pose more stringent requirements.

In order to achieve this, the following guidelines shall be observed:

- Any material proposed for use and which will be exposed to space vacuum should, at a minimum, pass the outgassing requirements TML≤1% and CVCM≤0.1% when tested according to ECSS-Q-ST-70-01C or ASTM-E595 (see section 6.5).
- Where possible, materials should be selected from ESA or NASA approved lists for space proven materials, such as ECSS-Q-70-71A RD[35] (even in such cases an outgassing test may be required, depending on the criticality of the processes involved, batch to batch variability, etc.).
- In specific cases a dynamic outgassing test, such as the ESA VBQC-test or the ASTM-E1559 (see section 6.5) is required. This should, at a minimum, be done if the material used covers a surface area larger than 1000 cm^2 (this also includes any MLI materials used).

6.7 Existing Tools and Databases

Several computer codes dedicated to spacecraft contamination exist. Most of them are simulation tools at system level, but some are devoted to thruster plume modelling. Some also contain integrated (limited) data bases.
The main field of applicability of the codes is external contamination in LEO or GEO orbit. However, some programs, have limited transport modelling capabilities (simple or improved view factors only), and will give poor results in cases when return-flux through self-scatter is important.
Many the tools are also capable of analysing semi-enclosed systems. Here again, some codes can be limited due to too poor transport modelling in case of high pressures. A difference with external contamination computing for which collisional return flux may often be the main contamination process (for surfaces not in direct view), is that in closed systems direct surface to surface collisionless transport (with possible surface reflections) is most of the time the dominant process. Except for really high pressures such as 10^{-3} hPa (and thus decimetric mean free path), which may be found in semi enclosed systems yet.

For a description of available tools see RD[1].

Some tools include data bases about contamination effects. References to some other important data bases created independent from the tools, are found in literature:

- A data base was created by Boeing Aerospace & Electronics in 1986-1988 for Air Force Wright Research and Development Centre RD[43]. Its availability to non-Americans is not reported. It is a very important work resulting from the collection of over 3000 sources and covering most of contamination fields.

- The Plume Contamination Database (PCD) was developed by MMS for ESTEC, using ORACLE RD[44]. It is anticipated that the database is progressively filled by ESTEC contractors and presently essentially contains measurements made at TUHH RD[45]. It should be available from ESA/ESTEC to the European space community.

These data bases can be used to assess contamination effects from contaminant deposit and column densities computed by the models described in the previous section.

7 REFERENCES

RD[1] ECSS-E-ST-10-04C Space Environment Standard
version linked to software tools is available at www.spenvis.oma.be/spenvis/

RD[2] SPENVIS – Space Environment Information System
http://www.spenvis.oma.be/spenvis/

RD[3] "Natural Orbital Environment Guidelines for Use in Aerospace Vehicle Development", B.J.Anderson, editor and R.E. Smith, compiler; NASA TM 4527, chapters 6 and 9, June 1994

RD[4] Nieminen P., "Spectral Input Code for Induced X-Ray Emission Calculations from Solar System Bodies", ESA Working Paper 2009, February 1999

RD[5] Evans S. W., "Natural Environment near the Sun/Earth-Moon L2 Libration Point", prepared for the Next Generation Space Telescope Program, NASA/MSFC, Tech Note 03009, Nov. 2003

RD[6] Grard R.J.L. and J.K.E.Tunaley, "Photo Electron Sheath Near a planar Probe in Interplanetary Space", J. Geophys.Res, 76, p.2498, 1971

RD[7] Huddleston D.E., A.D.Johnstone and A.J.Coates, "Determination of Comet Halley Gas Emission Characteristics from Mass Loading of the Solar Wind", J.Geophys.Res, 95, p.21, 1990

RD[8] Huebner W.F. and P.T.Giguere "A Model of Comet Comae II. Effects of Solar Photodissociative Ionization", Astrophys.J, 238, p.753, 1980

RD[9] Scialdone J.J. "An Estimate of the Outgassing of Space Payloads and Its Gaseous Influence on the Environment", J. Spacecraft and Rockets, 23, p.373, 1986

RD[10] Hess W.N., "The Radiation Belt and Magnetosphere", Blaisdell Publ. Co.,1968

RD[11] Daly, E.J., "The Radiation Belts", Radiation Physics and Chemistry 43, 1, pp.1-18 (in Special Issue on Space Radiation Environment and Effects), 1994

RD[12] Vette J.I. "The AE-8 Trapped Electron Model Environment", NSSDC/WDC-A-R&S Report 91-24, NASA-GSFC (1991)

RD[13] Sawyer D.M. and Vette J.I., "AP8 Trapped Proton Environment for Solar Maximum and Solar Minimum", NSSDC WDC-A-R&S 76-06, NASA-GSFC (1976).

RD[14] Probability Model for Cumulative Solar Proton Event Fluences, Xapsos, M. A., G.P. Summers, J.L. Barth, E. G. Stassinopoulos and E.A. Burke, IEEE Trans. Nucl. Sci., vol. 47, no. 3, June 2000, pp 486-490

RD[15] Feynman J., Spitale G., Wang J. and Gabriel S., "Interplanetary Proton Fluence Model: JPL 1991", J. Geophys. Res. 98, A8, 13281-13294 (1993).

RD[16] R. Mueller-Mellin, P. Nieminen , "Topical Teams in the Life & Physical Sciences", ESA SP-1281, pp 184-199

RD[17] King, J.H., "Solar Proton Fluences for 1977-1983 Space Missions", J. Spacecraft & Rockets 11, 401, (1974)

RD[18] Mathews J. and Towheed S., OMNIWeb, http://nssdc.gsfc.nasa.gov/omniweb/
mathews@nssdc.gsfc.nasa.gov, Code 633, NASA GSFC, Greenbelt, MD 20771, USA

RD[19] National Geophysical Data Center, "Space Environment Data from NOAA's GOES Satellites", National Geophysical Data Center, Code E/GC2, Dept. 946 325 Broadway Boulder Co 80303 3328 USA., also Space Physics Interactive Data Resource at http://www.ngdc.noaa.gov:8080/

RD[20] A.J. Tylka et al. "CREME96: A Revision of the Cosmic Ray Effects on Micro-Electronics Code", IEEE Trans. Nucl. Sci. NS-44, 2150-2160 (1997).

RD[21] Seltzer S., 'SHIELDOSE: A Computer Code For Space Shielding Radiation Dose Calculations', NBS Technical Note 1116, National Bureau of Standards, May 1980 .

RD[22] Geant4 Space Users: http://geant4.esa.int/

RD[23] G. Santin, V. Ivanchenko, H. Evans, P. Nieminen, E. Daly, "GRAS: A general-purpose 3-D modular simulation tool for space environment effects analysis", IEEE Trans. Nucl. Sci. 52, Issue 6, 2005, pp. 2294 – 2299. URL: http://space-env.esa.int/R_and_D/gras/

RD[24] MULASSIS implementation in SPENVIS : http://www.spenvis.oma.be/spenvis/help/models/mulassis.html

RD[25] Petersen E.L., "Approaches to Proton Single-Event-Rate Calculation", IEEE Trans. Nucl. Sci. NS-43, 2 (special issue on Single Event Effects and the Space Environment), 496 (1996)

RD[26] Pickel J.C., " Single-Event Effects Rate Prediction", IEEE Trans. Nucl. Sci. NS-43, 2 (special issue on Single Event Effects and the Space Environment), 483 (1996).

RD[27] R.A. Nymmik, M.I. Panasyuk, T. I. Pervaja, and A.A. Suslov "A Model of Galactic Cosmic Ray Fluxes", Nucl. Tracks & Radiat. Meas, 20, 427-429 (1992)

RD[28] J. Sorensen, "An Engineering Specification of the Internal Charging", Proceeding of the Symposium on Environment Modelling for Space-based Applications, ESA-SP-392, Dec. 1996

RD[29] Hopkinson G.R., Dale C.J. and Marshall P.W., "Proton Effects in Charge-Coupled Devices", IEEE Trans. Nucl. Sci. NS-43, 2 (special issue on Single Event Effects and the Space Environment), 614 (1996).

RD[30] Natural Orbital Environment Guidelines for Use in Aerospace Vehicle Development, Anderson B.J., by:, editor and R.E. Smith, compiler; NASA TM 4527, chapter 7, June 1994

RD[31] Collisional Balance of the Meteoritic Complex, Grün E., H.A. Zook, H. Fechtig and R.H. Giese, Icarus, Vol. 62, p.244, 1985

RD[32] MASTER 2005 DVD, ESA-SD-DVD-01, Release 1.0, April 2006

RD[33] ESABASE/DEBRIS, Meteoroid/Debris Impact Analysis, Technical Description G.Drolshagen and J.Borde, ref. ESABASE--GD--01/1, 1992

RD[34] ECSS-Q-ST-70-01C: Contamination and Cleanliness Control

RD[35] ECSS-Q-70-71A Data for selection of space materials and processes

RD[36] ASTM E-595 Standard test Method for Total Loss and Collected Volatile Condensable Materials from outgassing in a vacuum environment., http://www.astm.org/Standards/E595.htm

RD[37] ECSS-Q-ST-70-02C: Thermal vacuum outgassing test for the screening of space Materials

RD[38] ASTM E-1559 Standard test Method for contamination outgassing characteristics of space materials, http://www.astm.org/Standards/E1559.htm

RD[39] Scientific Foundations of Vacuum Technique, Dushman S.; Wiley & Sons, Inc, New-York-London

RD[40] Characterisation of the outgassing of spacecraft materials, Scialdone J.; SPIE Vol. 287 Shuttle Optical Environment; 1981

RD[41] Exhaust Plume Databook Update Version No 3 / ESA/ESTEC Contract 7590/87/NL/TP, Trinks H.

RD[42] Effect of Nozzle Boundary Layers on Rocket Exhaust Plumes, Simons G.A., AIAA Journal, Tech. Notes, vol.10, No 11, 1972, pp. 1534-1535

RD[43] Spacecraft contamination database, Thorton & Gilbert, SPIE Volume 13, 29; Optical System Contamination: Effects, Measurement and Control-2; 1990. pp 305-319

RD[44] PCD: An interactive tool for archiving plume impingement and contamination data, Chéoux-Damas P., Théroude C., Castejon S., Hufenbach B., The Proceedings of the Second European Spacecraft Propulsion Conference, ESTEC, Noordwijk, The Netherlands, May 27-29, 1997, p. 587-594

RD[45] Surface Effect Data Handbook (SEDH III), Report V, ESA Contract No 7510/87/NL/PP, Trinks H., Sept. 1991